Contents

1 Introduction

Providing one of the most precise experimental methods for Doppler-free measurements of lifetimes of excited states in atomic experiments, the Hanle effect is studied by determining the lifetime of excited $^3P_1$-state of mercury. With his classical interpretation of this phenomenon, Hanle contributed significantly to the replacement of the old quantum theory, which was unable to offer an adequate explanation of this effect. The interpretation of this effect spans both classical and quantum physics, therefore deepening the comprehension of the latter.

2 Theoretical Background

In the following section, both classical and quantum-mechanical theory of the Hanle effect is explained summarily. In addition, the theory of coherence narrowing and a possible methodical procedure to avoid this effect of artificial line narrowing are addressed.

2.1 Semi-Classical Interpretation

Classically, the Hanle effect can be established by the experimental setup displayed in fig. 1. A lamp produces light propagating in y-direction, which is parallelized by a lens and polarized in x-direction. In the origin of the used coordinate system, a mercury vapor containing cell is subjected to a uniform magnetic field B along the z axis.

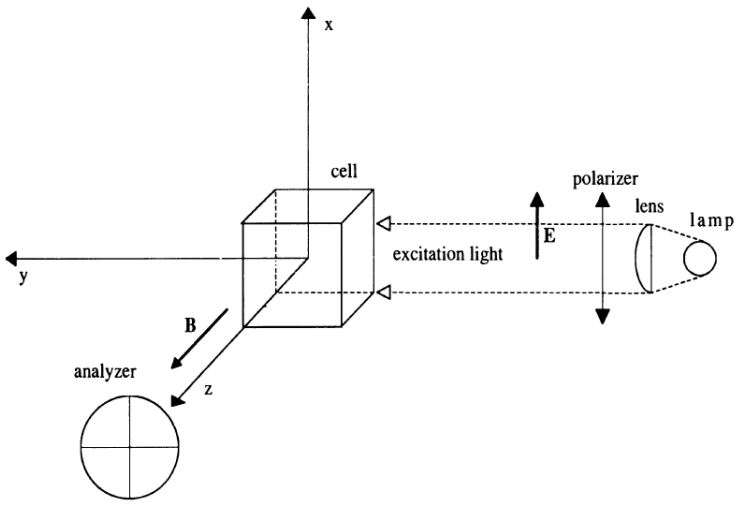

Figure 1: Experimental setup for the classical interpretation of the Hanle effect. The light wave, polarized in x direction, propagates in y direction and is absorbed by a mercury containing cell in the origin, subjected to a magnetic field $\boldsymbol{B} = B\hat{\boldsymbol{z}}$ parallel to the z-axis [1].

Due to the present magnetic field, the electrons of mercury-atoms precess in the $x, y-$ plane perpendicular to the magnetic field with the *Larmor* frequency ω_L

$$\omega_L = \frac{g_J \mu_B}{\hbar} B \tag{1}$$

where $\mu_B = \frac{e\hbar}{2m_e}$ is the Bohr magneton, and g_J the electronic g factor [2]. Those electrons can be considered as oscillating electric dipoles set along the x-axis. Since mechanical energy is converted into radiation energy, the electrons' motion is damped [3], which is represented pictorially in fig. 2 with increasing (left to right) field strengths.

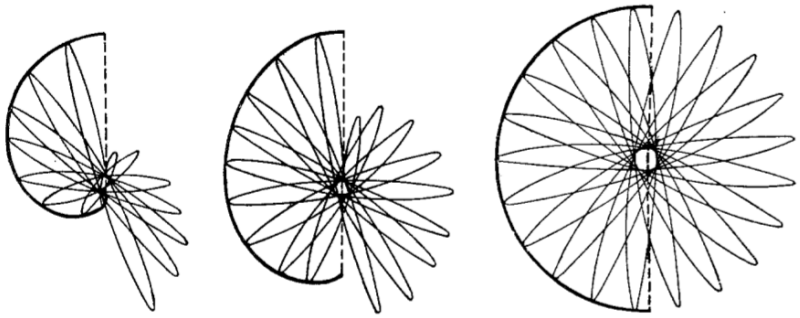

Figure 2: Precession of the electron bound to an atom, subjected to a magnetic field with increasing strength (from left to right, left: $T_{\mathrm{Orb}} < T_{\mathrm{Amp}}$, middle: $T_{\mathrm{Orb}} \sim T_{\mathrm{Amp}}$, right: $T_{\mathrm{Orb}} > T_{\mathrm{Amp}}$) [3].

For weak fields, the orbital period T_{Orb} is small compared to the period of fading of oscillation amplitude T_{Amp}. With higher field strength, the orbit period increases until the electron performs an undamped motion. Therefore it is expected, that depolarization of emitted light increases with the strength of magnetic field. Quantitatively, this intensity of radiation is characterized by a $\sin^2(\omega_L t)$ term, where $\theta(t) = \omega_L t$. The time dependent disexcitation of the electron into the ground state is represented by the phenomenological factor $\exp(-\frac{t}{\tau})$, with τ being the lifetime. Thus, the intensity I for a 90° angle between polarization direction and z-axis at $(\theta(0) = 0)$ leads according to [4] to

$$I = C \int_0^\infty e^{-\frac{t}{\tau}} \sin^2(\omega_L t) \mathrm{d}t = \frac{C\tau}{2} \left(\frac{(2\omega_L \tau)^2}{1 + (2\omega_L \tau)^2} \right) \tag{2}$$

Evaluation of this integral yields an inverted Lorentzian curve. The full width at half maximum ΔB of this curve can be converted to the full width at half maximum of the spectral line of the decaying state ΔE.

$$\Delta E = \hbar \omega_L (\Delta B) = g_J \mu_B \Delta B \tag{3}$$

Because of $\Delta E = \frac{\hbar}{\tau}$ with the lifetime τ of the decaying state, the lifetime is given by

$$\tau = \frac{\hbar}{g_J \mu_B \Delta B}. \tag{4}$$

If the polarization is perpendicular to the observation direction (0°) at the moment of absorption $(\theta(0) = \pi/2)$, then the intensity corresponds to a normal Lorentzian curve:

$$I = C \int_0^\infty e^{-\frac{t}{\tau}} \cos^2(\omega_L t) \mathrm{d}t = \frac{C\tau}{2} \left\{ 2 - \frac{(2\omega_L \tau)^2}{1 + (2\omega_L \tau)^2} \right\} \tag{5}$$

2.2 Quantum Mechanical Interpretation

Interpreted quantum mechanically, the Hanle effect depicts a special case of level crossing for the absence of a magnetic field $B = 0$. Consider an atom with the ground state a and two excited states b and c, connected to the ground state by allowed transitions. Those excited states can be degenerate by fine-structure splitting when no magnetic field is applied $B = 0$ or when there exist hyperfine multiplets with the same angular momentum $\boldsymbol{J}$. However, this degeneracy can be lifted, depending on the magnetic quantum number m_J, by applying a particular magnetic field B, inducing crossing of levels with increasing field strength [4] as seen in

fig. 3.

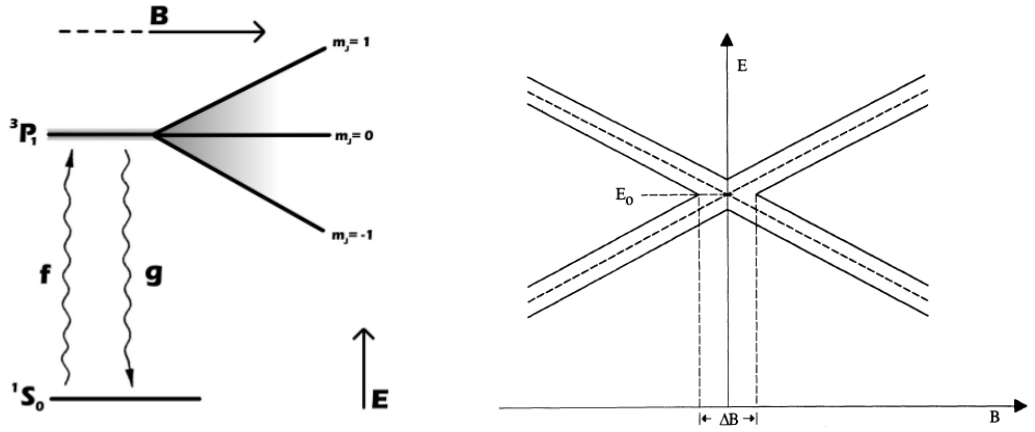

Figure 3: Energy level diagram of resonance fluorescence in mercury (left), with ground state $^1S_0$ and excited state $^3P_1$, which cross with increasing magnetic field B (right). Photons with polarization $\boldsymbol{f}$ are absorbed by the ground state, leading to excitation to the excited state. Even if excited states aren't crossed, simultaneous excitation to both states can happen, if $\Delta\nu$ is smaller than the Doppler-width of the light source. The disexcitation takes place under emission of $\boldsymbol{g}$ polarized light[5].

The states b and c, if close enough together, can be excited coherently. In the disexcitation process, interference effects occur and therefore more light is received by the detector used in fig. 1. In the case of the Hanle effect, the spectral resolution is limited mainly by the natural line width ($\sim \tau$, lifetime of the excited state) as well as pressure broadening ($\sim \ell$, mean free path). As in this experimental approach full attention is dedicated to the intensity I (which itself is not dependent on the energy), line broadening by Doppler-shift doesn't play any role. For a quantitative discussion, the rate R of absorbed photons with polarization $\boldsymbol{f}$ and re-emitted photons with polarization $\boldsymbol{g}$ is given by Breit [6]

$$R(\boldsymbol{f},\boldsymbol{g}) = C \sum_{\mu\mu' mm'} \frac{f_{\mu m} f_{m\mu'} g_{\mu' m'} g_{m'\mu}}{1 - 2\pi i \tau \nu(\mu,\mu')} \tag{6}$$

where c is a parameter containing geometrical factors as well as the intensity of incident light, μ, μ' are excited states, $\nu(\mu,\mu') = (E_\mu - E_{\mu'})/h$ the frequency difference of those excited states, $f_{\mu m} = \langle \mu | \boldsymbol{f} \cdot \boldsymbol{r} | m \rangle$ gives the probability of transition between two states μ and m, and τ is the mean lifetime of each excited state. When excited states are completely resolved, Breit's formula (eq. (6)) reduces to the case, where no interference is occurring:

$$R(\boldsymbol{f},\boldsymbol{g}) = c \sum_{\mu m m'} |f_{\mu m}|^2 |g_{\mu m'}|^2 = |f_{ab}|^2 |f_{ba}|^2 + |g_{ac}|^2 |g_{ca}|^2 \equiv R_0 \tag{7}$$

If the the excited states b and c are close enough together (see fig. 3) so that $2\pi\nu(\mu,\mu') \leq 1$, Breit's sum becomes continuous resulting in

$$R(\boldsymbol{f},\boldsymbol{g}) = R_0 + \frac{A}{1 - 2\pi i \nu(b,c)} + \frac{A^*}{1 + 2\pi i \nu(b,c)} \equiv R_0 + S \tag{8}$$

with the term $A = f_{ba} f_{ac} g_{ca} g_{ab}$ depending on the angles between polarization, field, beam as well as observation direction. Thus, the signal term S can be rewritten to

$$S = \frac{A + A^*}{1 + 4\pi^2 \tau^2 \nu^2(b,c)} + \frac{(A - A^*) 2\pi i \tau \nu(b,c)}{1 + 4\pi^2 \tau^2 \nu^2(b,c)} \tag{9}$$

Thus, following cases can be considered

- If $A \in \mathbb{R}$, then S is Lorentzian with full width $\Delta\nu(b,c) = 1/(\pi\tau) = g_J\mu_B\Delta B/(\pi\hbar)$ in accordance with the classical result, seen in eq. (4)
- If $A \in \mathbb{C} : \mathfrak{Re}(A) = 0$, then $S = \frac{4\pi i A\tau\nu(b,c)}{1+4\pi^2\tau^2\nu^2(b,c)}$ with characteristic dispersion shape
- If $A \in \mathbb{C} : \mathfrak{Re}(A) \neq 0$, then mixture of those cases above can be observed

2.3 Coherence Narrowing

Coherence narrowing occurs if an atom is excited by a photon emitted by a disexciting atom. Following the argumentation presented in section 2.1, both atoms, the initial excited by external light and the atom excited by a photon produced in the disexcitation process, perform the same precession. The second atom disexcites under emission of a photon with the same phase, polarization and direction as the initial photon. This process happens multiple times at sufficient scattering cross sections and sufficient densities. The observed lifetime appears therefore to be longer, which directly transfers to the FWHM of the registered intensity signal I. However, this effect can be cancelled by measuring the lifetime for various densities ρ of the gas. By extrapolation against the density $0\,\mathrm{kg/m^3}$, the case with nearly no other atoms present is simulated, resulting in the undisturbed lifetime. Though the density is not an accessible observable of this experiment, yet it is known that the seeming prolongation of lifetime depends exponentially on the temperature T, which indeed is an observable in this setup, and linearly on the pressure p of the system. The pressure of the mercury vapor can be determined at known temperature T from

$$\ln\left(\frac{p}{p_c}\right) = \frac{T_c}{T}\left(a_1T_r + a_2T_r^{1.89} + a_3T_r^2 + a_4T_r^8 + a_5T_r^{8.5} + a_6T_r^9\right) \tag{10}$$

where $T_r = 1 - T/T_c$ and T_c being the critical temperature and p_c the critical pressure. The exponents used are validated both theoretically and using numerical models for real gases [4].

3 Experimental Setup and Procedure

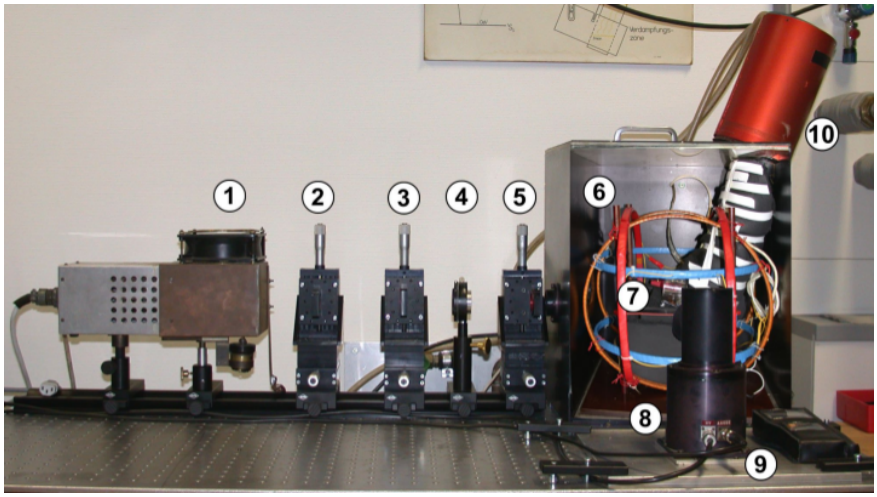

Figure 4: Experimental setup of the Hanle experiment, with mercury vapor-lamp (1), lenses (2 and 5), interference filter (3), polarization filter (4), resonance cell storing the liquid mercury (6) in a lightproof box (8, not shown), Peltier elements (10) for cooling of the cell via heat-pipes (not indicated), Helmholtz coils (7) and photomultiplier (9) [4].

Since the disexcitation of the $^3P_1$ state of mercury into the ground state $^1S_0$ takes place under emission of 253.7 nm wavelength photons, a high-frequency voltage operated cooled mercury vapour-lamp (1, see fig. 4) is used as a light source in this setup. The course of the beam is thereupon parallelized and focused by two lenses (2 and 5). In between those lenses, a narrow wavelength-range of (255 ± 5)nm FWMH is selected using an interference filter (3). Control over the polarization direction is taken with a polarization filter (4). Liquid mercury, which is subject of this investigation, is deposited in a cavity of a quartz-glass piston.

The cooling unit consists of four water-cooled Peltier elements (10) controlled by a constant current generator. The heat is transported by freon containing heat-pipes which are in contact with the quartz cell through an oil bath surrounded by a copper block. Three pairs of Helmholtz coils (7) with 56 windings each surround the cell. Two of those ($y, z-$direction) compensate the surrounding magnetic field. The other pair ($x-$direction) is employed in order to create the Zeeman splitting, generating the Hanle-signal. Using a ramp generator, a linear rising voltage is applied to this pair of Helmholtz-coils. The produced fluorescence signal is guided by an aluminium pipe perpendicular to the beamline to a photomultiplier (9). Both Peltier elements and photomultiplier are placed further away of the Helmholtz coils in order to minimize disturbing effects by external fields. The output current of the photomultiplier is amplified and converted to a voltage signal by an externally powered ampèremeter. This voltage signal is displayed with the voltage of the ramp enerator on an oscilloscope.

The Hanle signal is measured with an oscilloscope at various temperatures T of the system, for three polarizer settings $\alpha \in \{0°, 45°, 90°\}$ each. To ensure a stable environment, measurements have been held on for 20 minutes after changing the temperature. According to theory, the Hanle signal is produced if and only if the magnetic field is zero. Therefore, the coil current is run linearly from -1 A up to 1 A using a ramp generator. In order to take into account known hysteresis effects of the temperature of the mercury containing cell, a measurement series both for heating and cooling of the cell is taken.

4 Evaluation

The evaluation of the Hanle curves is performed using `python3`, especially for curve fitting the modules `scipy.stats` and `scipy.optimize` are employed. In order to evite repetition, explicit analysis is only shown for representative Hanle signals of each polarizer setting and measurement mode. The source code including the full analysis of all taken data sets is attached to this protocol in appendix A.

4.1 Hanle Signal Analysis

In order to obtain results in desired units, the gradient m of the voltage of the ramp generator, as depicted in fig. 5, is determined exemplarily for one data set using a linear model $f_{\text{Linear}}(t; m, b)$.

$$f_{\text{Linear}}(t; m, b) = m \cdot t + b \tag{11}$$

The uncertainty s_t on the time has been estimated to one increment, since the set time divisions remained unchanged throughout all measurements, this time-uncertainty equals to $s_t = 0.02\,\text{s}$. With a Pearson-R value of 0.997, the voltage gradient resulting from linear analysis is $m = (1.542 \pm 0.003)\,\text{V/s}$.

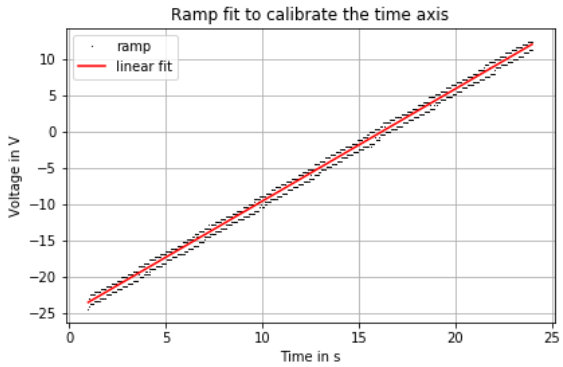

Figure 5: Linear fit of voltage of ramp generator for calibration of time, yielding a voltage gradient of $m = (1.542 \pm 0.003)\,\text{V/s}$ with a Pearson-R of 0.997.

For the main analysis of the Hanle signal, the following general Lorentzian model $f_{\text{Lorentzian}}$ as a function of time t is considered

$$f_{\text{Lorentzian}}(t; p_1, p_2, p_3, p_4) = \frac{2p_1}{\pi} \cdot \frac{p_2}{4(t - p_3)^2 + p_2^2} + p_4 \tag{12}$$

where p_1 is the area under the Lorentzian curve, p_2 the FWHM, p_3 refers to the position of the extremum and p_4 is the general offset of the whole signal. All parameters p_i are obtained from a least squares fit, for which the initial values p_{i_0}have been set by hand. The fitted Hanle signals for 0° and 90° at $T_{\text{heating}} = -17°\text{C}$ are shown in figs. 6a and 6b and at $T_{\text{cooling}} = -11°\text{C}$ in figs. 6c and 6d respectively. The remainder of fitted Hanle signals is found in appendix C.

From this model, the full width at half maximum intensity p_2 can be extracted directly in units of time. Prior to the determination of lifetime τ, a unit conversion of the FWHM p_2 from time (in s) to magnetic field strength (in T) is made. Herefore, a one-to-one current to voltage conversion and amplification by a factor of $k = 10$ by the oscilloscope is assumed [4]. For

conversion to the magnetic field strength, the geometry factor $B_{\text{calib}} = 3.363 \times 10^{-4}\,\text{T/A}$ [4] of the used coils is taken into account. Thus, conversion of the state variables' units is given by

$$\Delta B = m \cdot k \cdot B_{\text{calib}} \cdot p_2$$

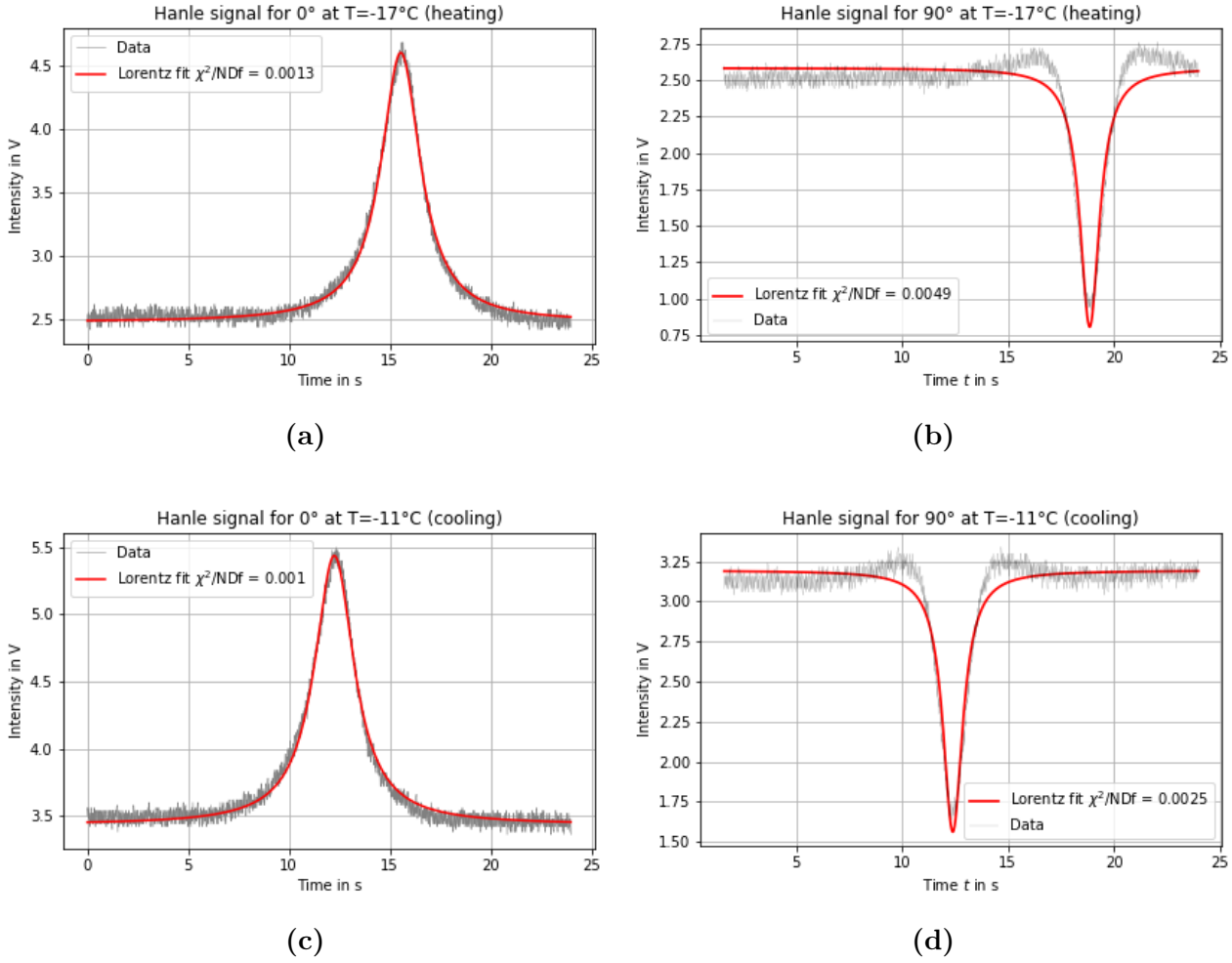

Figure 6: Hanle signals (gray) at $T = -17°\text{C}$ (heating; a,b) as well as for $T = -11°\text{C}$ (cooling; c,d) for polarizer settings 0° (a,c) and 90° (b,d) with fit of Lorentzian function (red). Lifetime τ is determined from FWHM of fitted Lorentzian.

Herefrom, the lifetime τ of the excited $^3P_1$-state of Hg is determined by eq. (4)

$$\tau = \frac{\hbar}{g_J \mu_B \Delta B}$$

where the theoretical value of $g_J = 1.5$ for the excited state of interest, and the experimental values of $\mu_B = 9.274\,009 \times 10^{-24}\,\text{J/T}$ and $\hbar = 1.054\,571\,8 \times 10^{-34}\,\text{Js}$ are used. Since the relative error of those constants is negligible in direct comparison with the remaining uncertainties of the slope s_m and the FWHM s_{p_2}, the general uncertainty on the lifetime s_τ is obtained from Gaussian error propagation.

$$s_\tau^{\text{gen}} = \tau \cdot \sqrt{\left(\frac{s_m}{m}\right)^2 + \left(\frac{s_{p_2}}{p_2}\right)^2}$$

The lifetime is determined for polarizer angles $\alpha \in \{0°, 90°\}$ and both measurement modes, heating and cooling, at various temperatures T. The final results are given in tables 1 and 2.

Polarizer α	0°		90°	
T in °C	τ_0 in ns	χ^2_0/NDf	τ_{90} in ns	χ^2_{90}/NDf
−17	61.3±0.4	0.0013	130.4±2.5	0.004
−16	60.7±0.5	0.0018		
−14	60.9±0.5	0.0010	121.7±2.1	0.003
−12	59.6±0.5	0.0011	120.4±2.1	0.003
−9	61.6±0.5	0.0012	119.1±2.0	0.003
−7	60.5±0.5	0.0012	127.9±2.8	0.005
−6	59.7±0.5	0.0010	120.5±2.0	0.003
−5	60.8±0.5	0.0010	130.7±2.8	0.004
−2	61.0±0.5	0.0009		
2	60.5±0.5	0.0009	125.8±2.4	0.003
5	60.6±0.4	0.0008	127.9±2.3	0.002
7	61.1±0.5	0.0008	133.1±2.8	0.003
10	60.2±0.5	0.0008	130.4±2.4	0.002

Table 1: Optimization results for 0° and 90° at heating mode for various temperatures T yielding the lifetime τ of excited $^3P_1-$state of mercury using eq. (4). Herefore, the FWHM necessary for further calculation is obtained from least squares analysis of the Hanle signal.

Polarizer α	0°		90°	
T in °C	τ_0 in ns	χ^2_0/NDf	τ_{90} in ns	χ^2_{90}/NDf
−11	61.1±0.5	0.0010	128.8±2.2	0.003
−8	60.2±0.5	0.0009	134.3±2.7	0.003
−6	55.3±1.8	0.0183	134.7±2.6	0.002
−4	61.4±0.5	0.0007	136.0±3.0	0.002
−3	61.5±0.6	0.0009	138.4±3.0	0.002
−2	60.0±0.6	0.0008	141.2±3.6	0.002
0	61.3±0.6	0.0009	138.5±3.4	0.001
1	58.8±0.6	0.0009	140.3±3.5	0.002
2	59.0±0.7	0.0009	144.2±4.1	0.002
4	61.5±0.9	0.0010	146.4±5.1	0.002
9	57.2±0.9	0.0009	144.2±4.9	0.001
12	57.4±0.9	0.0009	146.8±5.5	0.001
14	68.0±1.1	0.0007	144.3±6.9	0.001
15	58.3±1.2	0.0006	153.0±7.3	0.001

Table 2: Optimization results for 0° and 90° at cooling mode for various temperatures T. The lifetime τ of excited $^3P_1-$state of mercury is obtained using eq. (4), where the converted and scaled FWHM retrieved from least squares analysis is used.

To relate the uncertainty on the lifetime s_τ^{gen} from above, multiple measurements of the Hanle signals for both polarizer settings 0° and 90° at constant temperature have been made (as seen in appendices A and C), yielding following average statistical uncertainties

$$s_{\tau_0}^{\text{stat}} = 0.43\,\text{ns}$$
$$s_{\tau_{90}}^{\text{stat}} = 0.88\,\text{ns}$$

Therefore, the total uncertainty s_τ is obtained by Gaussian error propagation for absolute uncertainties

$$s_\tau = \sqrt{\left(s_\tau^{\text{gen}}\right)^2 + \left(s_\tau^{\text{stat}}\right)^2} \tag{13}$$

45° Polarization

The Hanle signal for 45° polarization is shown for one temperature exemplarily in fig. 7. It looks like a dispersion curve as expected. No further evaluation, which means computation of lifetime, of the 45° Hanle signals is performed because of the suboptimal symmetry of the measured signals.

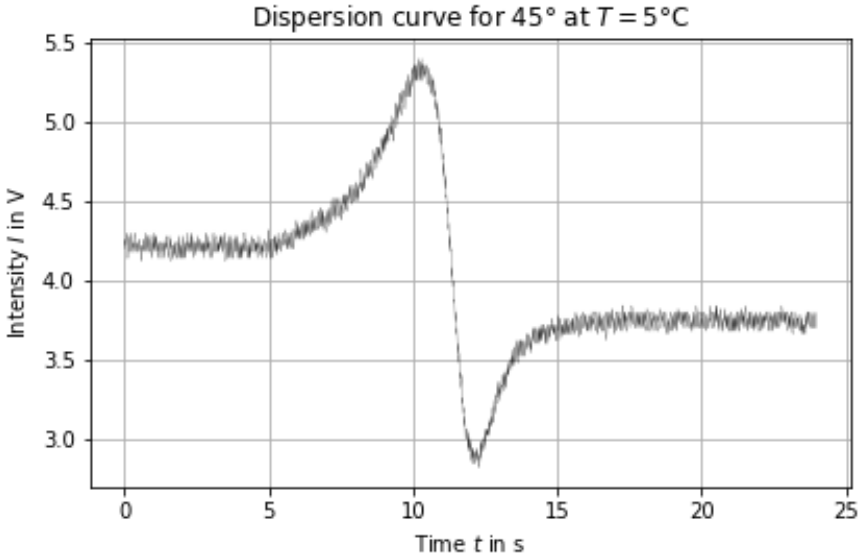

Figure 7: The Hanle signal for 45° polarization at $T = 5\,°\text{C}$ in the heating process shows the expected course of a dispersion curve.

4.2 Correction of Lifetime

Corrections of narrowing of width of the intensity spectrum due to re-absorption of photons emitted during disexcitation of mercury atoms are carried out by extrapolation. By coherence narrowing, the measured lifetime seems to be prolonged. This prolongation depends exponentially on the temperature T and linearly on the pressure p. Therefore, the lifetime is set as a function of pressure, where conversion has been made using eq. (10) with parameters a_i given in [4], $T_c = 1764\,\text{K}$ and $p_c = 167\,\text{MPa}$ (see figs. 8a to 8d). With `numpy.polyfit()`, a linear regression of the obtained lifetimes has been carried out. The corrected lifetime τ_{cor} is given by the y-axis intercept of the linear fit. For both polarization angles, we obtain following corrected lifetimes

$$\begin{aligned}
\tau_0^{\text{heating}} &= (60.7 \pm 0.5)\,\text{ns} \\
\tau_0^{\text{cooling}} &= (60.4 \pm 0.9)\,\text{ns} \\
\tau_{90}^{\text{heating}} &= (123 \pm 2)\,\text{ns} \\
\tau_{90}^{\text{cooling}} &= (134 \pm 2)\,\text{ns}
\end{aligned}$$

Here, the lifetime uncertainty s_τ is determined as the square root of the sum of squared individual statistical and general uncertainties given in eq. (13). The uncertainty s_p on the pressure is obtained by Gaussian error propagation with input (statistical) uncertainty of $s_T = 1\,\mathrm{K}$ on the temperature. The uncertainties of the given parameters $a_1 - a_6$ are neglected.

$$s_p = p{\cdot}s_T \left[-\frac{T_c}{T^2} \cdot \left(a_1 T_r + a_2 T_r^{1.89} + a_3 T_r^2 + a_4 T_r^8 + a_5 T_r^{8.5} + a_6 T_r^9 \right) + \frac{1}{T} \left(a_1 + 1.89 \cdot a_2 T_r^{0.89} + 2 \cdot a_3 T_r + 8 \cdot a_4 T_r^7 + 8.5 \cdot a_5 T_r^{7.5} + 9 \cdot a_6 T_r^8 \right) \right]$$

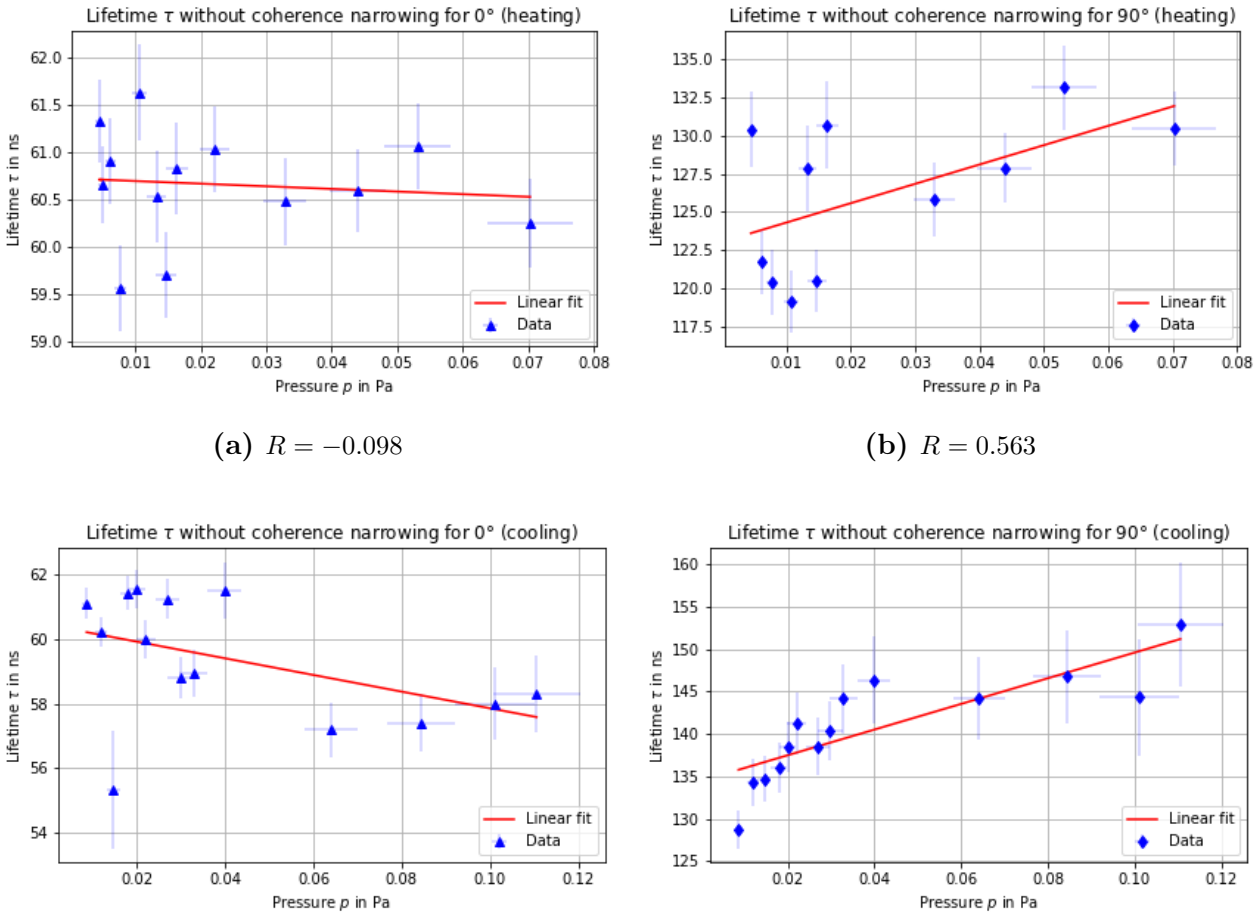

(a) $R = -0.098$ **(b)** $R = 0.563$

(c) $R = -0.451$ **(d)** $R = 0.826$

Figure 8: Correction of determined lifetimes τ (blue) from coherence narrowing for heating (a,b) and cooling (c,d) processes and polarizer settings 0° (a,c) and 90° (b,d). Corrected lifetimes are determined as the offset τ_{cor} of a linear fit (red) with displayed Pearson-R obtained from linear regression with `numpy.polyfit()`.

5 Summary and Discussion

In this experiment, the lifetime τ of the excited $^3P_1$-state of mercury has been determined. Therefor, the Hanle signal at polarizer angles 0°, 45° and 90° has been measured for various temperatures. This procedure was performed both for heating and cooling of the mercury cell, in order to take account of possible hysteresis effects of the cooling system. The lifetime τ has been determined for polarizer angles 0° and 90°. Therefor, the full width at half maximum of measured Hanle signals is obtained from fitting Lorentzian curves to the measured intensity. The Lorentzian nature of measured Hanle signals can be confirmed taking into account the calculated reduced χ^2 values.

With a linear regression, the obtained lifetimes (set as a function of pressure p) have been corrected from coherence narrowing. Therefor, the measured temperatures have been converted to pressures. Extrapolation to $p = 0\,\mathrm{Pa}$ yielded the corrected lifetimes τ_{cor}, summarized in table 3. For this part of the analysis, both systematic and statistic uncertainties on the lifetime have been considered. A general dependence of the lifetime on the measurement mode (heating and cooling) is observable. This effect can be explained taking into account the setup of the resonance cell, consisting of materials with different heat conductivities. The temperature sensor has been integrated underneath the copper block. Due to its higher heat conductivity, the reaction to temperature changes of copper is relatively fast, such that a further systematic uncertainty has to be taken into account because the temperature of the copper block was measured and not directly the temperature of the mercury, which reacts more slowly to temperature changes. However, only the 90° measurement yields results of the same order as the literature value of 119 ns given in [4]. Here, the corrected lifetimes show a 2σ (heating) and 6σ (cooling) deviation from the literature value. The systematic deviation of both lifetimes can be seen as a result of the temperature issue explained above.

	Corrected Lifetime τ_{cor} in ns	
Process	0° polarization	90° polarization
heating	60.7 ± 0.5	123 ± 2
cooling	60.4 ± 0.9	134 ± 2
Average	61 ± 1	129 ± 3

Table 3: Corrected lifetimes τ_{cor} for both polarizer settings 0° and 90° and measuring modes, obtained from the y-axis intercepts of linear fits given in fig. 8.

For 0° polarization, neither a general trend due to coherence narrowing, nor a reasonable corrected lifetime is obtained. The computed lifetimes rise with decreasing pressure which is contrarious to the theoretical expectations due to assumed reabsorption of resonance fluorescence light. Since the systematic uncertainties rooted in the temperature measurement are the same for 90° polarization angle, we assume polarization-dependent influences of one or more of the components used in this setup. A possible polarization dependency of the used interference filter is conceivable, since the absolute intensity (amplitude of Hanle signal) of both polarizer settings are differing. Furthermore, an age-related wearing of the used cell, and thus deviations in pressure of the mercury-vapor resonance cell, is assumed as a possible source of error.

List of Figures

List of Tables

References

[1] Bergou, Beverini, Gawlik, et al. *The Hanle Effect and Level-Crossing Spectroscopy*. Springer Science + Business Media, LLC, 1991.

[2] R. L. deZafra and W. Kirk. Measurement of the atomic lifetime by the hanle effect. *American Journal of Physics*, 35(7):573–582, 1967.

[3] W. Hanle. *Über magnetische Beeinflussung der Polarisation von Resonanzfluoreszenz*. Dissertation, Universität Göttingen, 1924.

[4] M. Köhli, M. Gessner, and S. Fischer. Der hanle-effekt. Fortgeschrittenen praktikum i versuchsanleitung, Albert-Ludwigs-Universität Freiburg, 2011.

[5] P.A. Franken. Interference effects in the resonance fluorescence of "crossed" excited atomic states. *Physical Review*, 121(2):508–512, January 1961.

[6] G. Breit. Quantum theory of dispersion. *Review of modern Physics*, 5(2):91–137, April 1933.

A Source Code

Due to the extreme length of the source code, the source code of the analysis is given in a separate file, accessible via Hanle_Eval_Group120.pdf.

B Measurement Journal

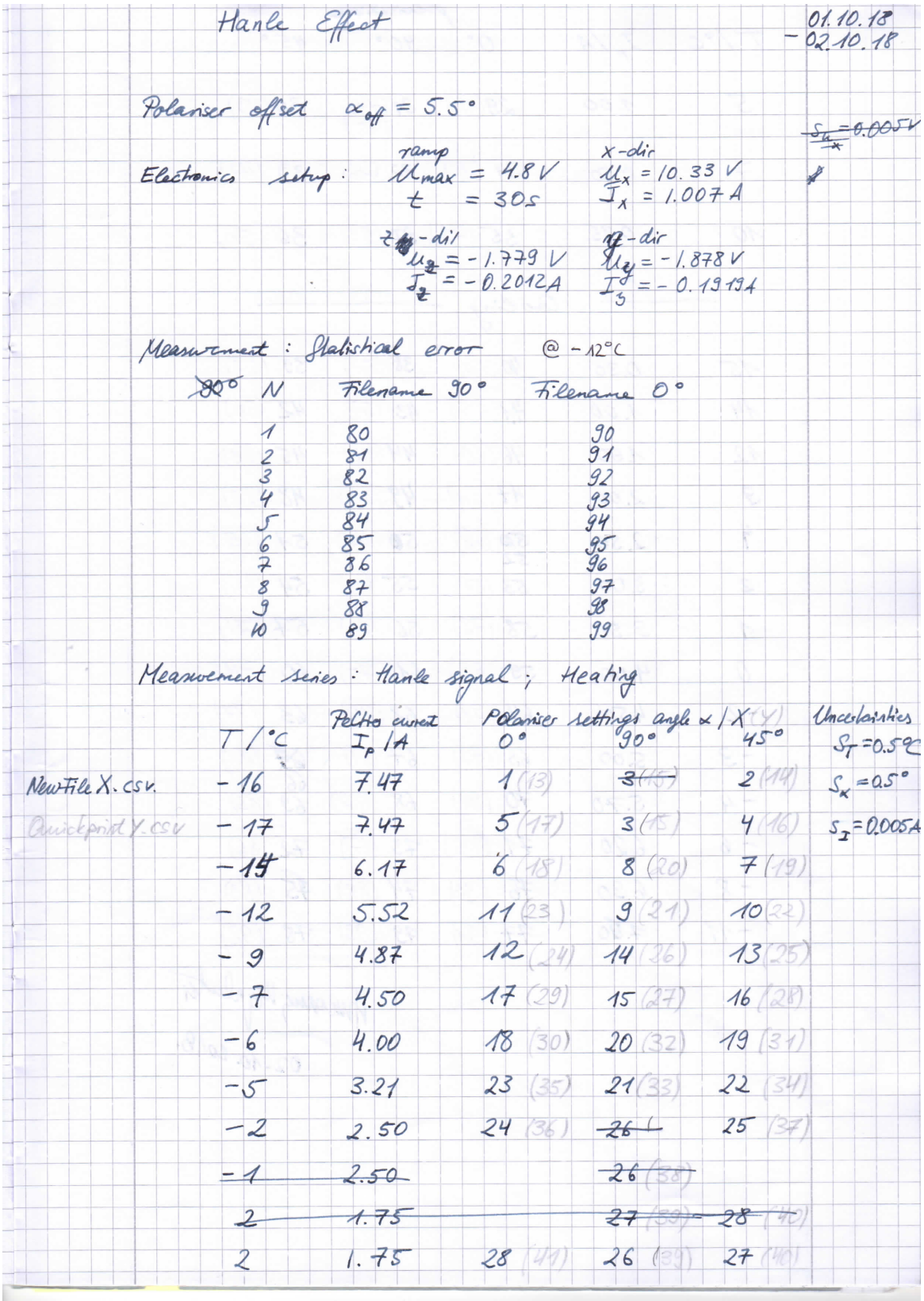

Hanle Effect

01.10.18
– 02.10.18

Polariser offset $\alpha_{off} = 5.5°$

Electronics setup:
ramp: $U_{max} = 4.8\,V$, $t = 30\,s$
x-dir: $U_x = 10.33\,V$, $I_x = 1.007\,A$
z-dir: $U_z = -1.779\,V$, $I_z = -0.2012\,A$
y-dir: $U_y = -1.878\,V$, $I_y = -0.19191\,A$

Measurement: Statistical error @ –12°C

N	Filename 90°	Filename 0°
1	80	90
2	81	91
3	82	92
4	83	93
5	84	94
6	85	95
7	86	96
8	87	97
9	88	98
10	89	99

Measurement series: Hanle signal; Heating

	T / °C	Peltier current I_p / A	Polariser settings angle α / X (Y) 0°	90°	45°
NewFile X.csv	–16	7.47	1 (13)	~~3 (15)~~	2 (14)
Quickprint Y.csv	–17	7.47	5 (17)	3 (15)	4 (16)
	~~–15~~	6.17	6 (18)	8 (20)	7 (19)
	–12	5.52	11 (23)	9 (21)	10 (22)
	–9	4.87	12 (24)	14 (26)	13 (25)
	–7	4.50	17 (29)	15 (27)	16 (28)
	–6	4.00	18 (30)	20 (32)	19 (31)
	–5	3.21	23 (35)	21 (33)	22 (34)
	–2	2.50	24 (36)	~~26~~	25 (37)
	~~–1~~	~~2.50~~		~~26 (38)~~	
	~~2~~	~~1.75~~		~~27 (39)~~	~~28 (40)~~
	2	1.75	28 (41)	26 (39)	27 (40)

Uncertainties
$S_T = 0.5°C$
$S_x = 0.5°$
$S_I = 0.005A$

Figure 9: Measurement journal page 1

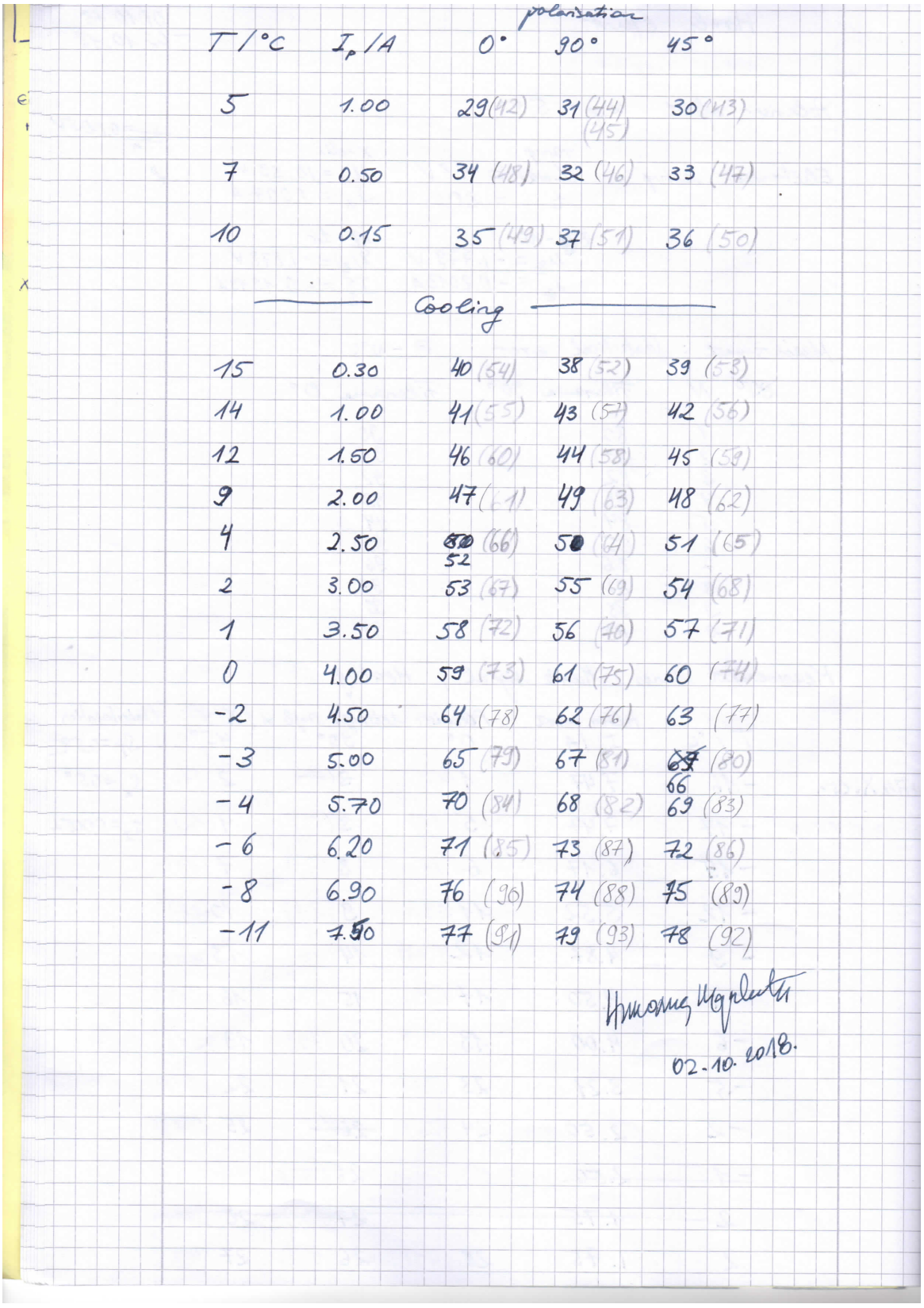

T / °C	I_p / A	polarisation 0°	90°	45°
5	1.00	29 (42)	31 (44) (45)	30 (43)
7	0.50	34 (48)	32 (46)	33 (47)
10	0.15	35 (49)	37 (51)	36 (50)
		Cooling		
15	0.30	40 (54)	38 (52)	39 (53)
14	1.00	41 (55)	43 (57)	42 (56)
12	1.50	46 (60)	44 (58)	45 (59)
9	2.00	47 (61)	49 (63)	48 (62)
4	2.50	~~50~~ 52 (66)	50 (64)	51 (65)
2	3.00	53 (67)	55 (69)	54 (68)
1	3.50	58 (72)	56 (70)	57 (71)
0	4.00	59 (73)	61 (75)	60 (74)
-2	4.50	64 (78)	62 (76)	63 (77)
-3	5.00	65 (79)	67 (81)	~~69~~ 66 (80)
-4	5.70	70 (84)	68 (82)	69 (83)
-6	6.20	71 (85)	73 (87)	72 (86)
-8	6.90	76 (90)	74 (88)	75 (89)
-11	7.50	77 (91)	79 (93)	78 (92)

02.10.2018.

Figure 10: Measurement journal page 2

C Additional plots

C.1 0° polarization

C.1.1 Heating

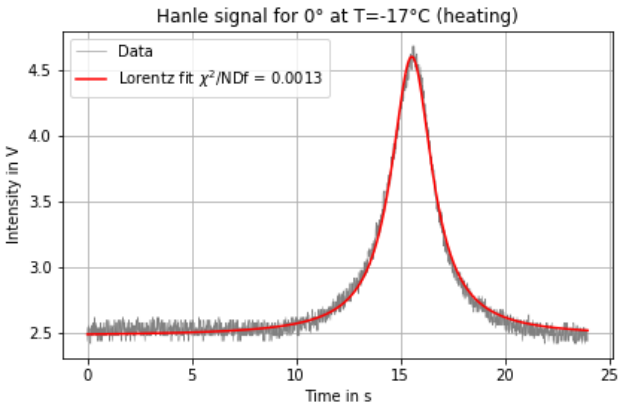

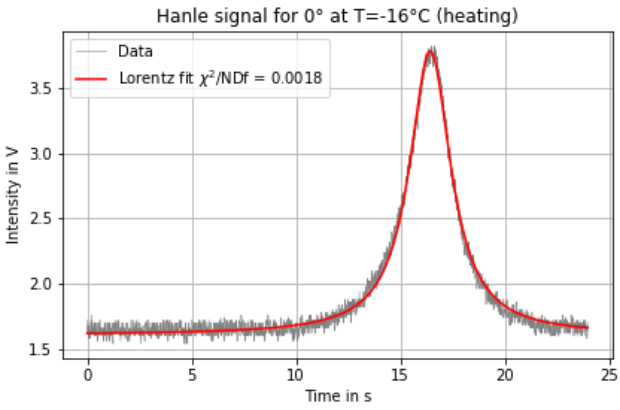

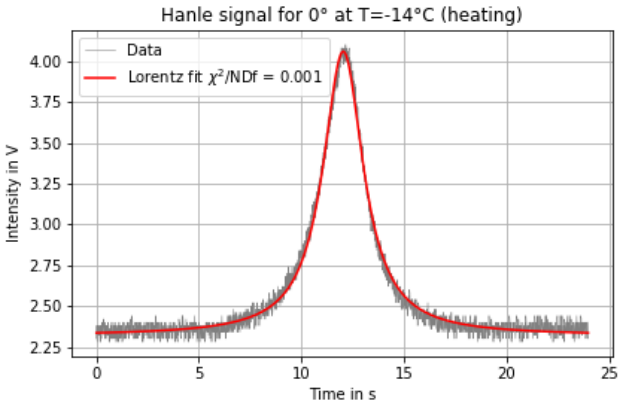

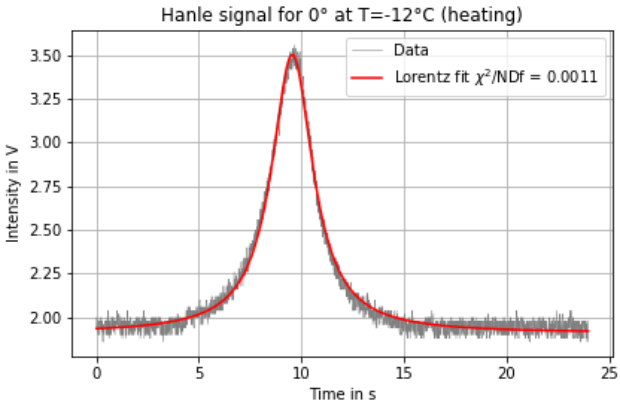

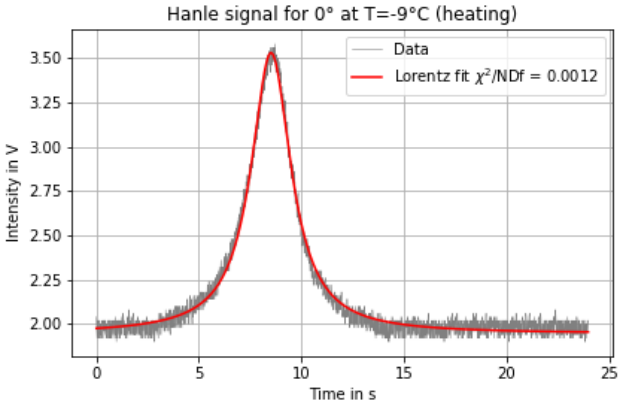

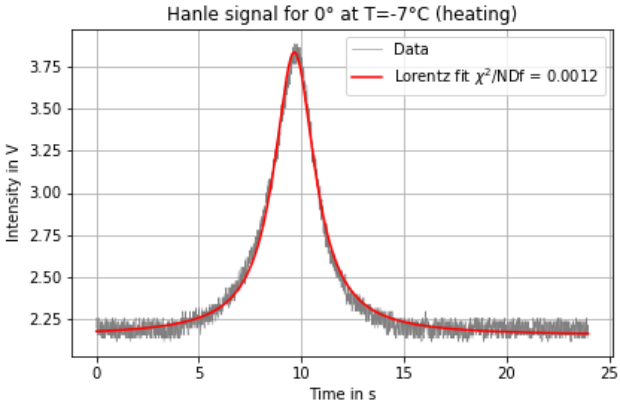

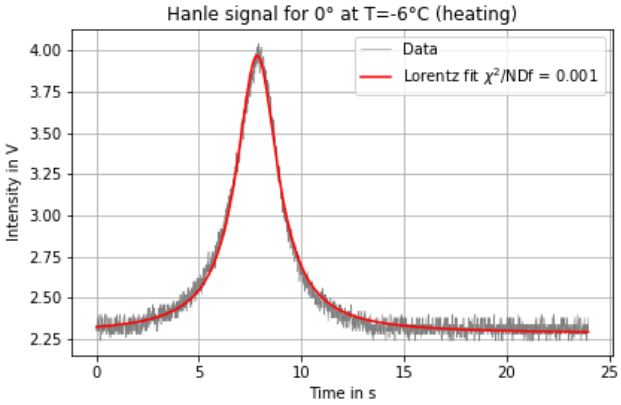
Hanle signal for 0° at T=-6°C (heating)
Data
Lorentz fit χ^2/NDf = 0.001
Intensity in V
Time in s

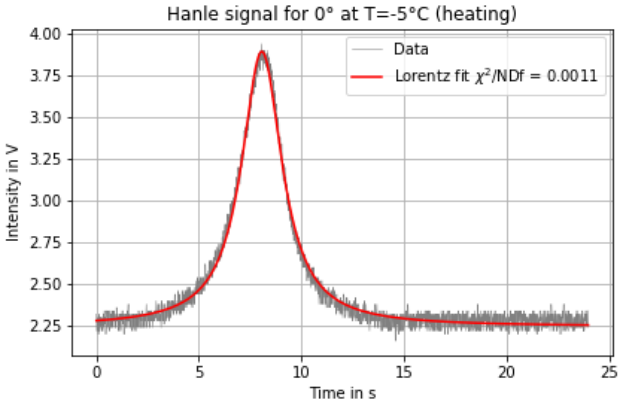
Hanle signal for 0° at T=-5°C (heating)
Data
Lorentz fit χ^2/NDf = 0.0011
Intensity in V
Time in s

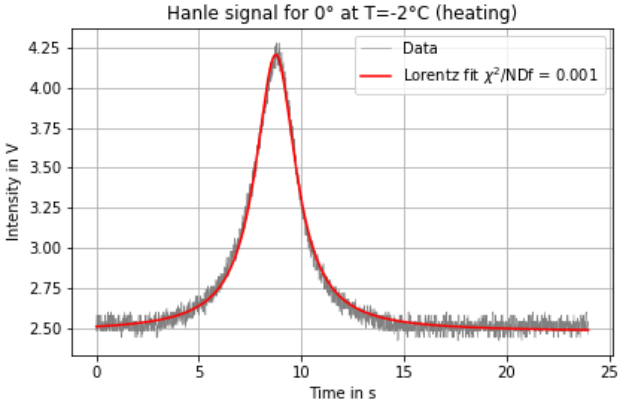
Hanle signal for 0° at T=-2°C (heating)
Data
Lorentz fit χ^2/NDf = 0.001
Intensity in V
Time in s

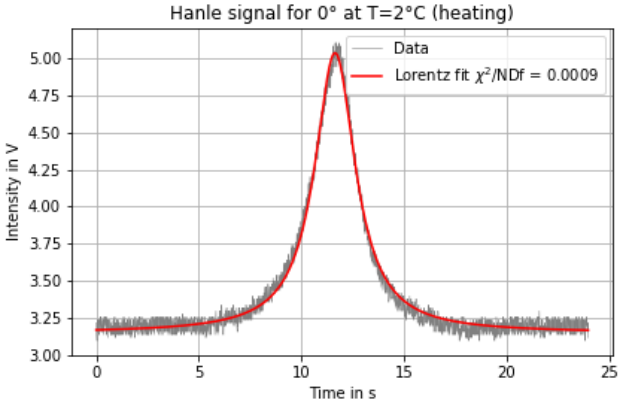
Hanle signal for 0° at T=2°C (heating)
Data
Lorentz fit χ^2/NDf = 0.0009
Intensity in V
Time in s

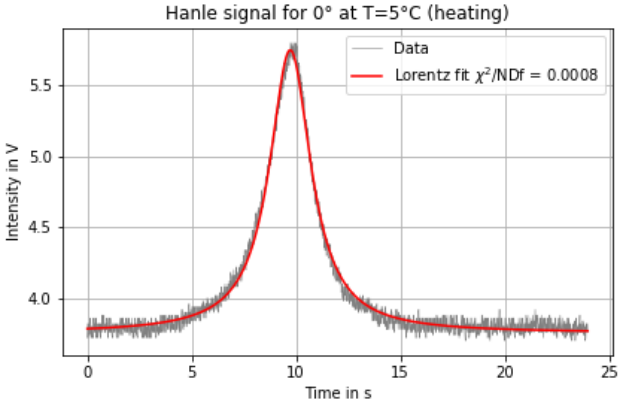
Hanle signal for 0° at T=5°C (heating)
Data
Lorentz fit χ^2/NDf = 0.0008
Intensity in V
Time in s

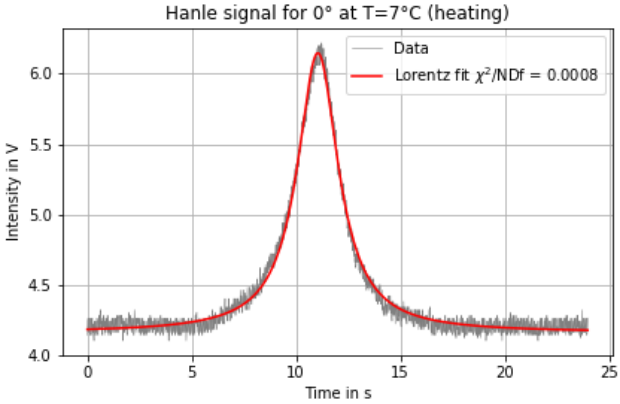
Hanle signal for 0° at T=7°C (heating)
Data
Lorentz fit χ^2/NDf = 0.0008
Intensity in V
Time in s

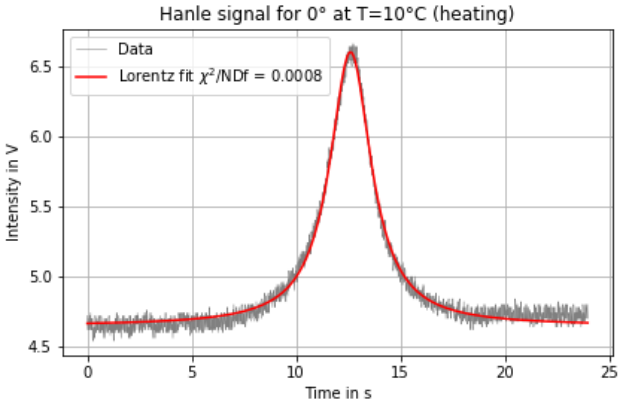
Hanle signal for 0° at T=10°C (heating)
Data
Lorentz fit χ^2/NDf = 0.0008
Intensity in V
Time in s

C.1.2 Cooling

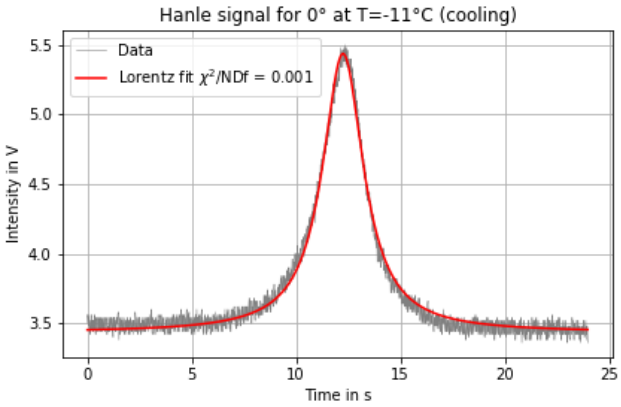
Hanle signal for 0° at T=-11°C (cooling)
Data
Lorentz fit χ^2/NDf = 0.001
Intensity in V
Time in s

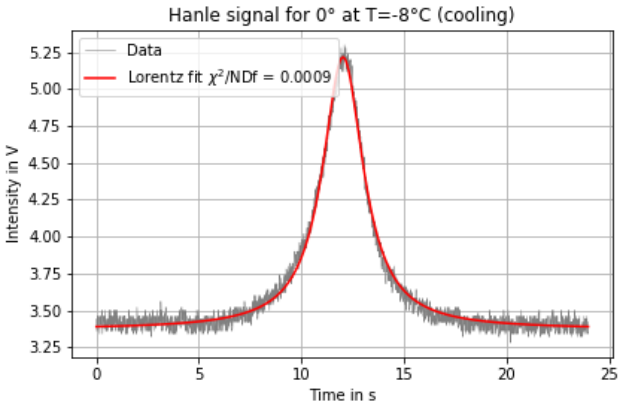
Hanle signal for 0° at T=-8°C (cooling)
Data
Lorentz fit χ^2/NDf = 0.0009
Intensity in V
Time in s

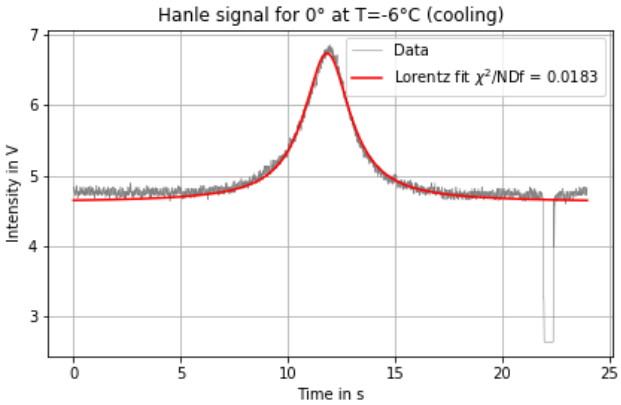
Hanle signal for 0° at T=-6°C (cooling)
Data
Lorentz fit χ^2/NDf = 0.0183
Intensity in V
Time in s

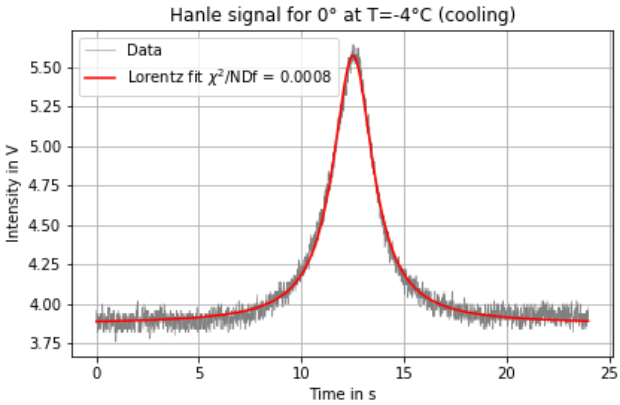
Hanle signal for 0° at T=-4°C (cooling)
Data
Lorentz fit χ^2/NDf = 0.0008
Intensity in V
Time in s

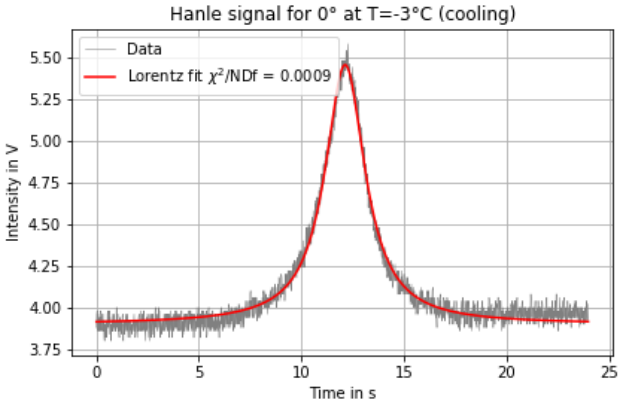
Hanle signal for 0° at T=-3°C (cooling)
Data
Lorentz fit χ^2/NDf = 0.0009
Intensity in V
Time in s

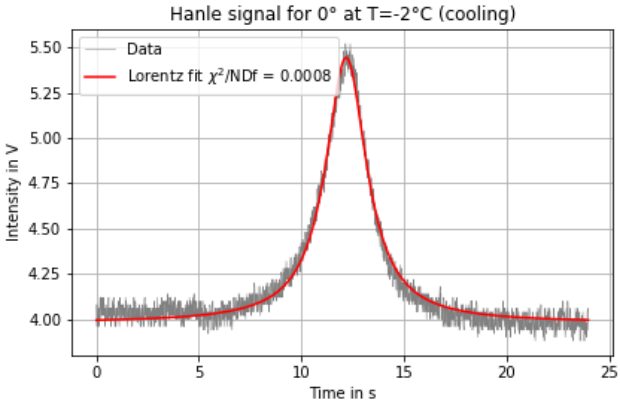
Hanle signal for 0° at T=-2°C (cooling)
Data
Lorentz fit χ^2/NDf = 0.0008
Intensity in V
Time in s

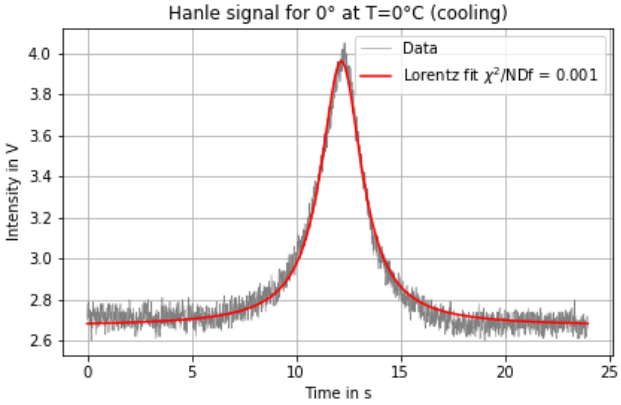
Hanle signal for 0° at T=0°C (cooling)
Data
Lorentz fit χ^2/NDf = 0.001
Intensity in V
Time in s

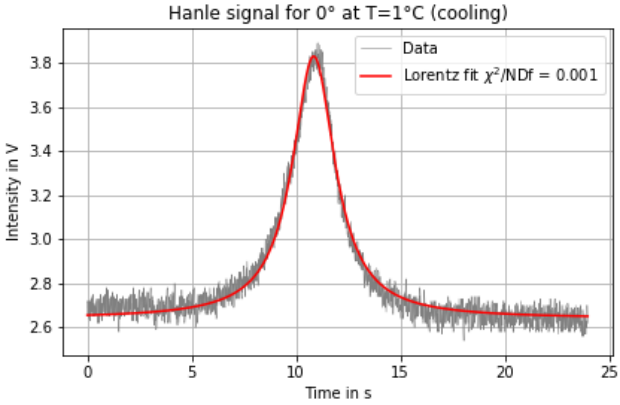
Hanle signal for 0° at T=1°C (cooling)
Data
Lorentz fit χ^2/NDf = 0.001
Intensity in V
Time in s

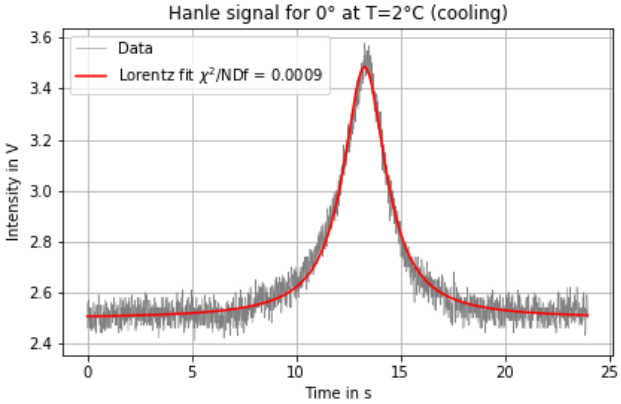
Hanle signal for 0° at T=2°C (cooling)
Data
Lorentz fit χ^2/NDf = 0.0009
Intensity in V
Time in s

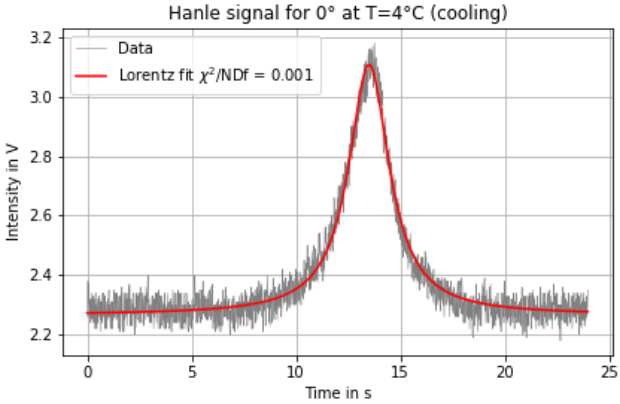
Hanle signal for 0° at T=4°C (cooling)
Data
Lorentz fit χ^2/NDf = 0.001
Intensity in V
Time in s

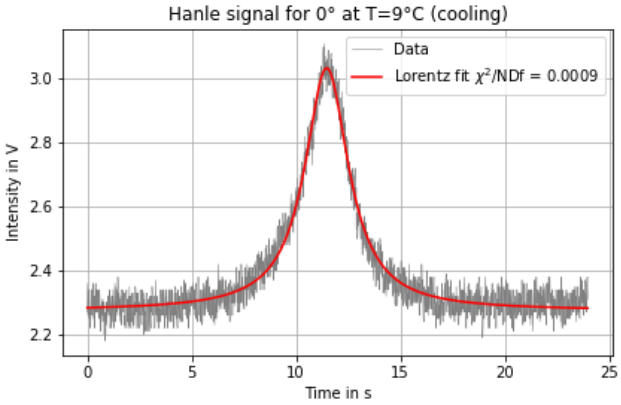
Hanle signal for 0° at T=9°C (cooling)
Data
Lorentz fit χ^2/NDf = 0.0009
Intensity in V
Time in s

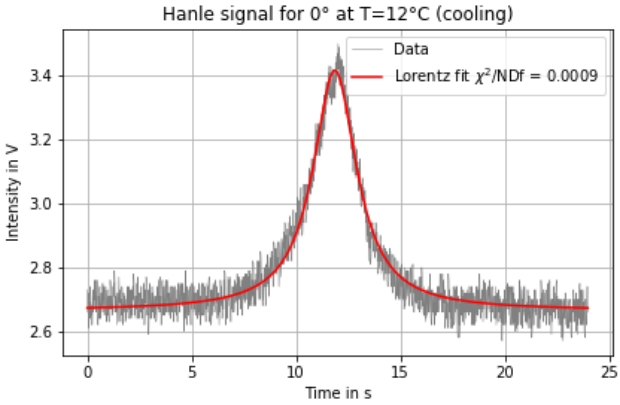
Hanle signal for 0° at T=12°C (cooling)
Data
Lorentz fit χ^2/NDf = 0.0009
Intensity in V
Time in s

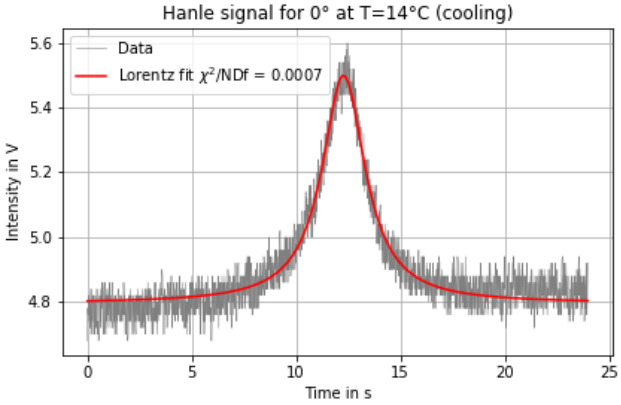
Hanle signal for 0° at T=14°C (cooling)
Data
Lorentz fit χ^2/NDf = 0.0007
Intensity in V
Time in s

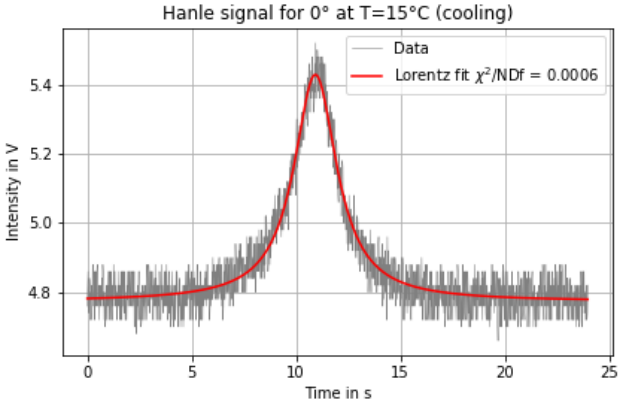
Hanle signal for 0° at T=15°C (cooling)
Data
Lorentz fit χ^2/NDf = 0.0006
Intensity in V
Time in s

C.1.3 Statistical Measurement

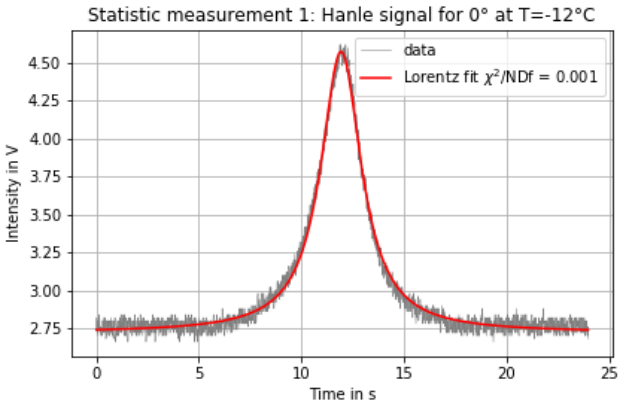

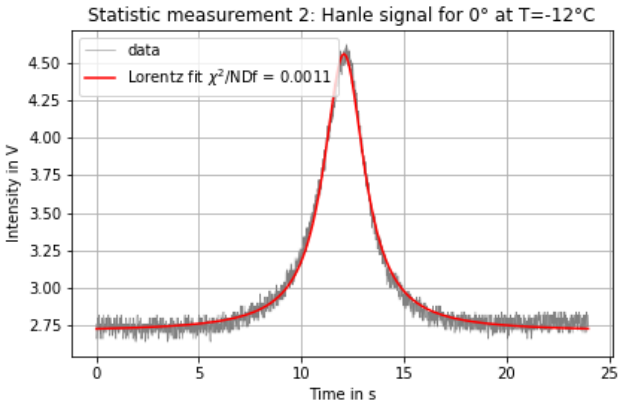

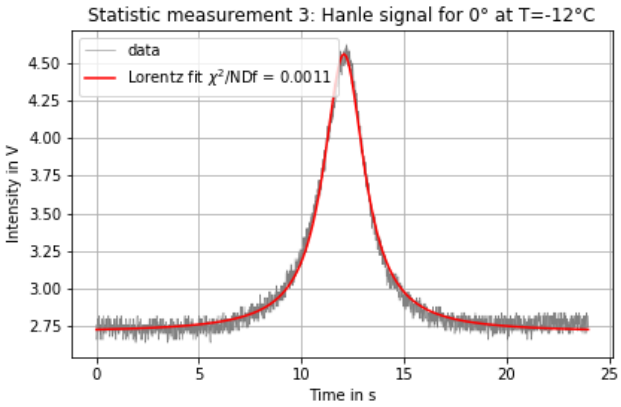

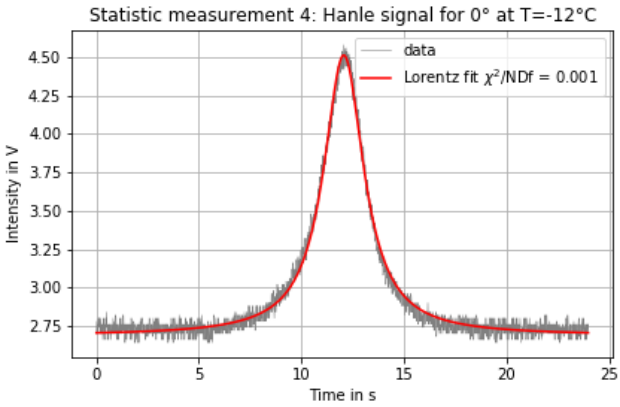

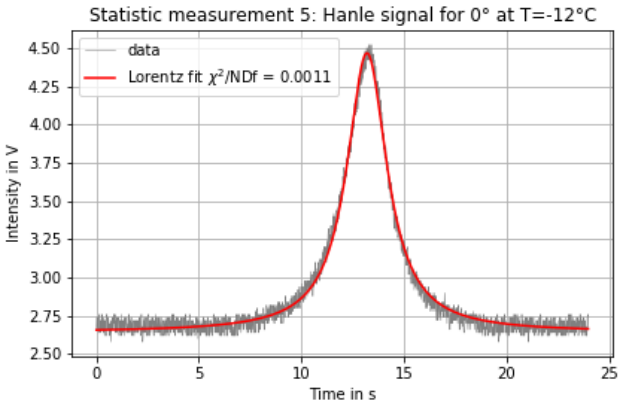

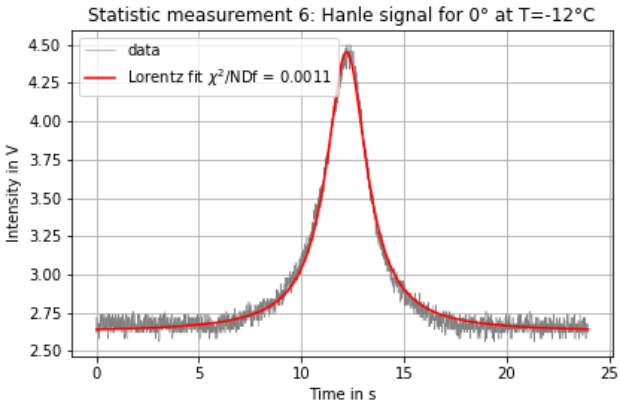

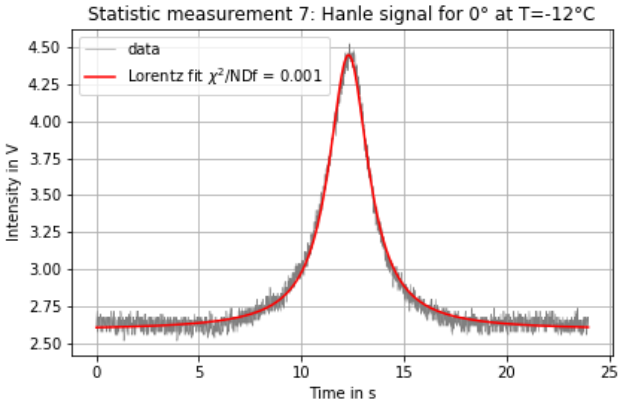
Statistic measurement 7: Hanle signal for 0° at T=-12°C
data
Lorentz fit χ^2/NDf = 0.001
Intensity in V
Time in s

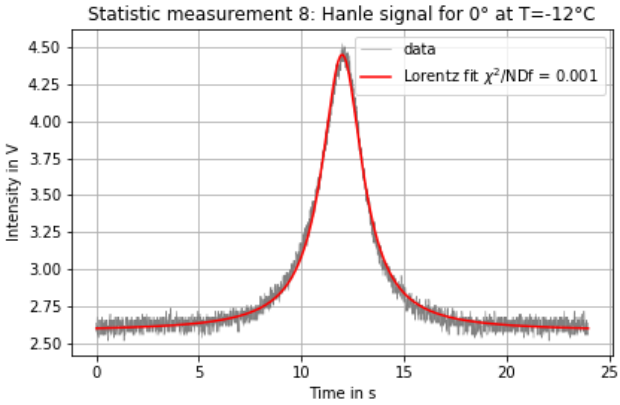
Statistic measurement 8: Hanle signal for 0° at T=-12°C
data
Lorentz fit χ^2/NDf = 0.001
Intensity in V
Time in s

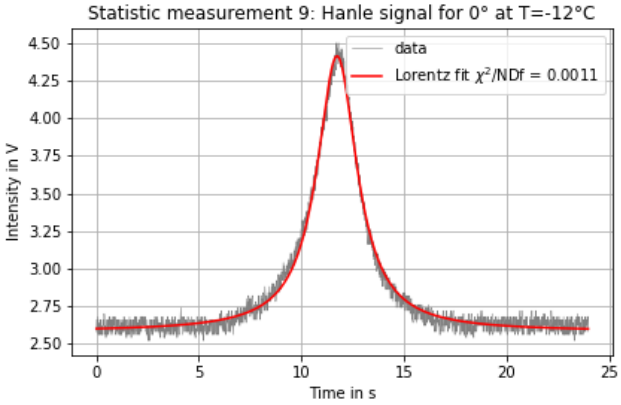
Statistic measurement 9: Hanle signal for 0° at T=-12°C
data
Lorentz fit χ^2/NDf = 0.0011
Intensity in V
Time in s

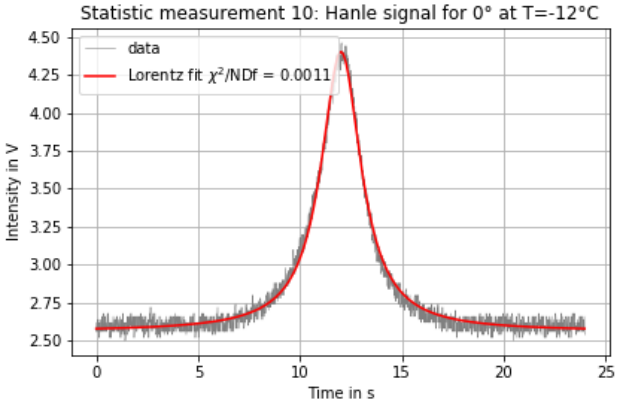
Statistic measurement 10: Hanle signal for 0° at T=-12°C
data
Lorentz fit χ^2/NDf = 0.0011
Intensity in V
Time in s

C.2 90° polarization

C.2.1 Heating

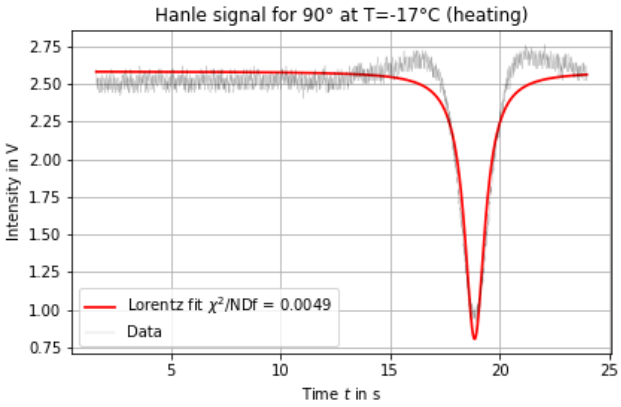

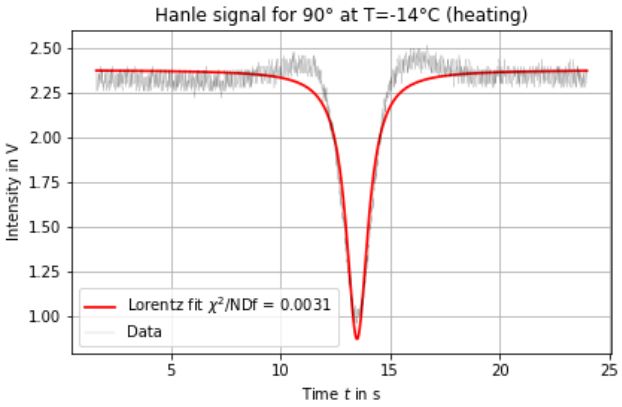

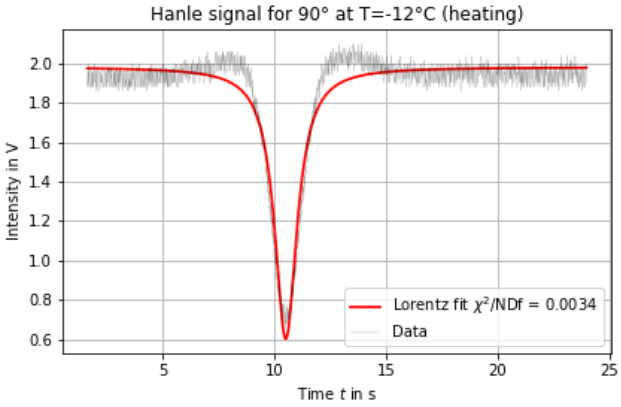

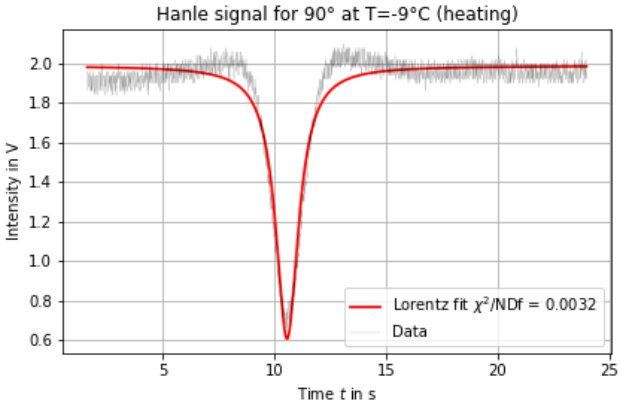

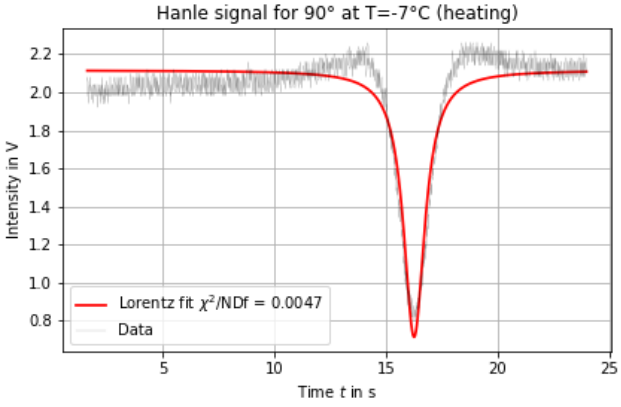

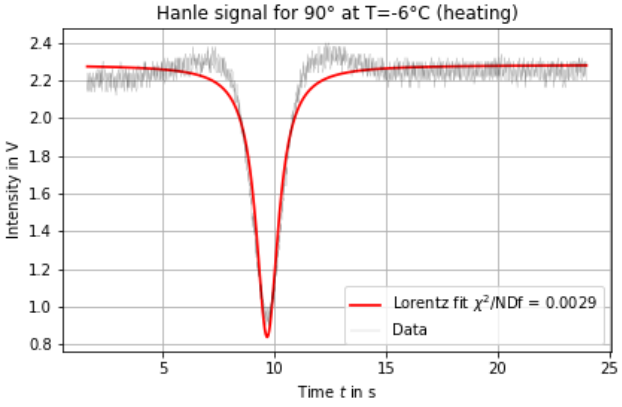

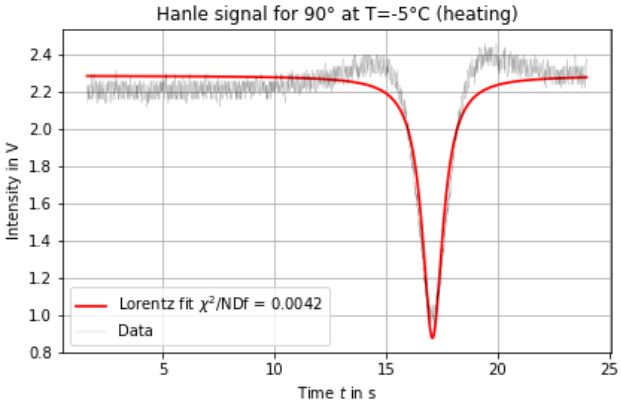
Hanle signal for 90° at T=-5°C (heating)
Intensity in V
Time t in s
Lorentz fit χ^2/NDf = 0.0042
Data

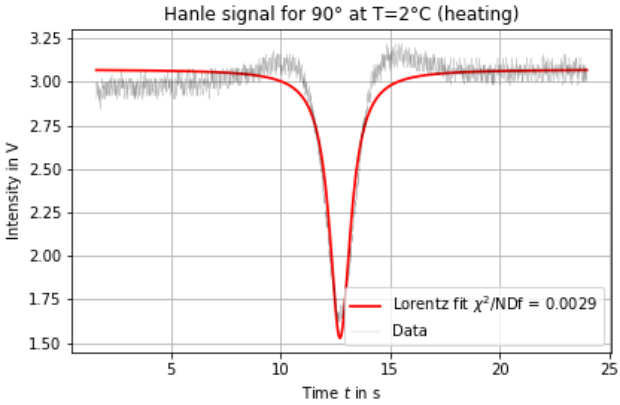
Hanle signal for 90° at T=2°C (heating)
Intensity in V
Time t in s
Lorentz fit χ^2/NDf = 0.0029
Data

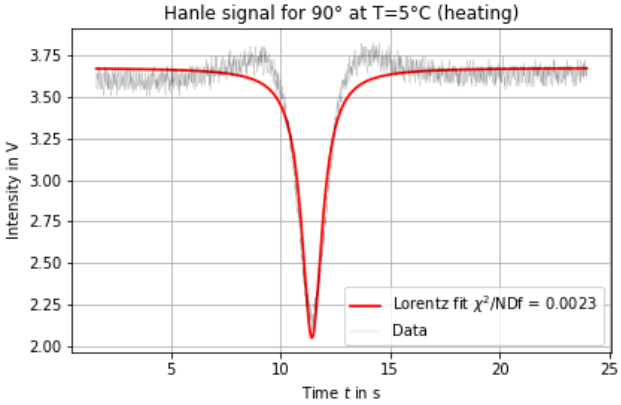
Hanle signal for 90° at T=5°C (heating)
Intensity in V
Time t in s
Lorentz fit χ^2/NDf = 0.0023
Data

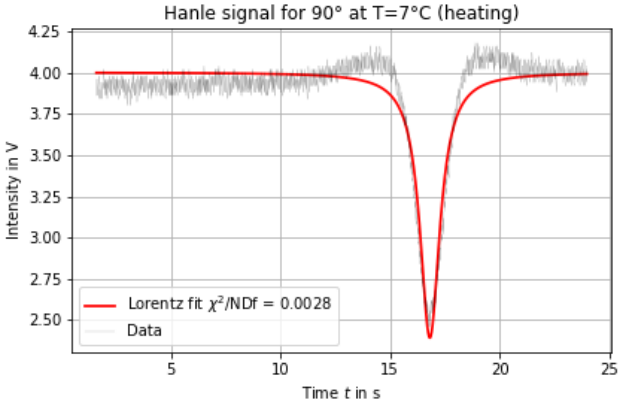
Hanle signal for 90° at T=7°C (heating)
Intensity in V
Time t in s
Lorentz fit χ^2/NDf = 0.0028
Data

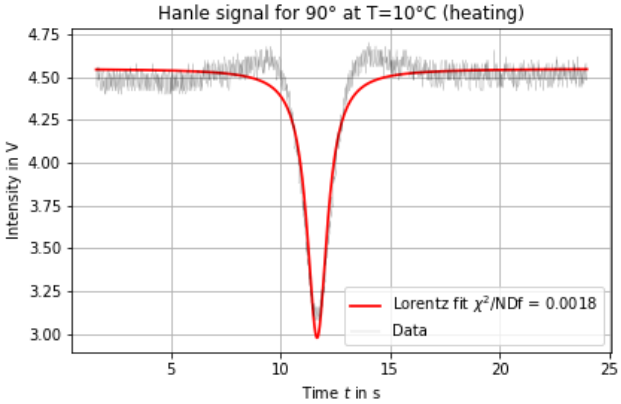
Hanle signal for 90° at T=10°C (heating)
Intensity in V
Time t in s
Lorentz fit χ^2/NDf = 0.0018
Data

C.2.2 Cooling

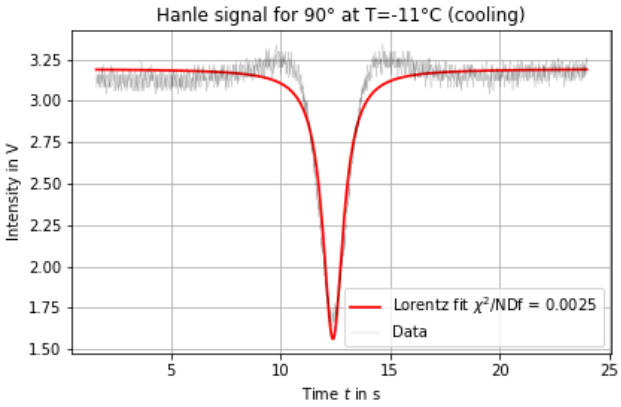
Hanle signal for 90° at T=-11°C (cooling)
Intensity in V
Time t in s
Lorentz fit χ^2/NDf = 0.0025
Data

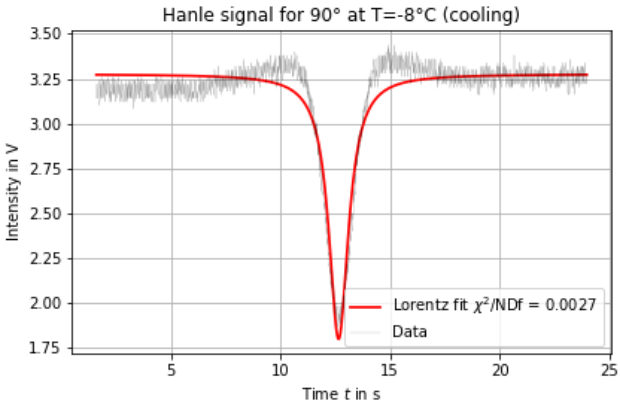
Hanle signal for 90° at T=-8°C (cooling)
Intensity in V
Time t in s
Lorentz fit χ^2/NDf = 0.0027
Data

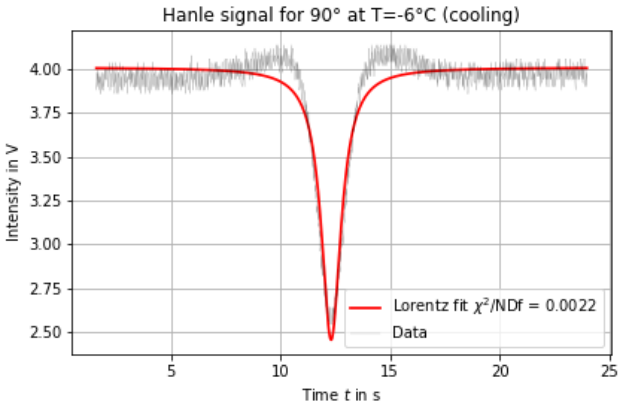
Hanle signal for 90° at T=-6°C (cooling)
Intensity in V
Time t in s
Lorentz fit χ^2/NDf = 0.0022
Data

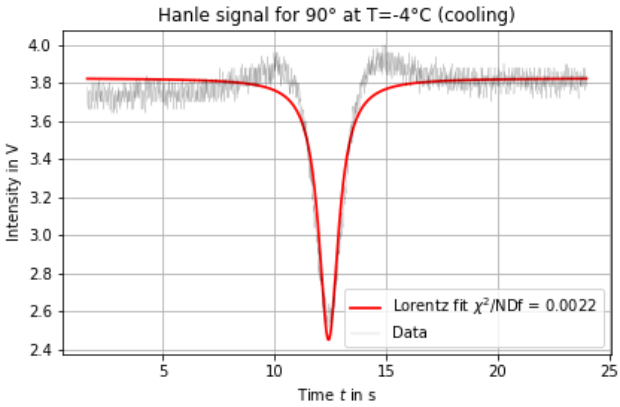
Hanle signal for 90° at T=-4°C (cooling)
Intensity in V
Time t in s
Lorentz fit χ^2/NDf = 0.0022
Data

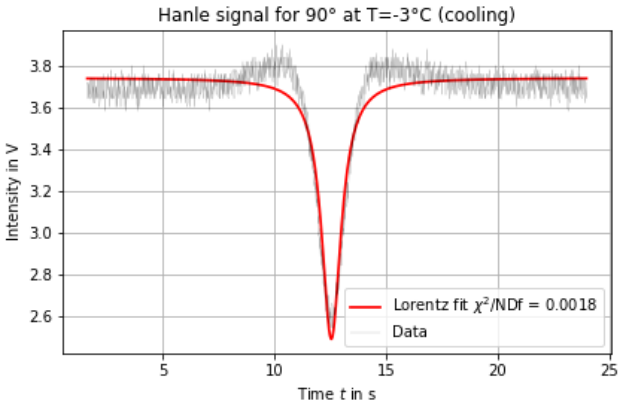
Hanle signal for 90° at T=-3°C (cooling)
Intensity in V
Time t in s
Lorentz fit χ^2/NDf = 0.0018
Data

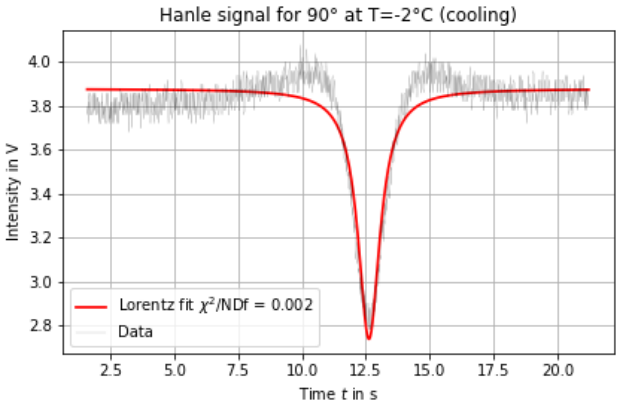
Hanle signal for 90° at T=-2°C (cooling)
Intensity in V
Time t in s
Lorentz fit χ^2/NDf = 0.002
Data

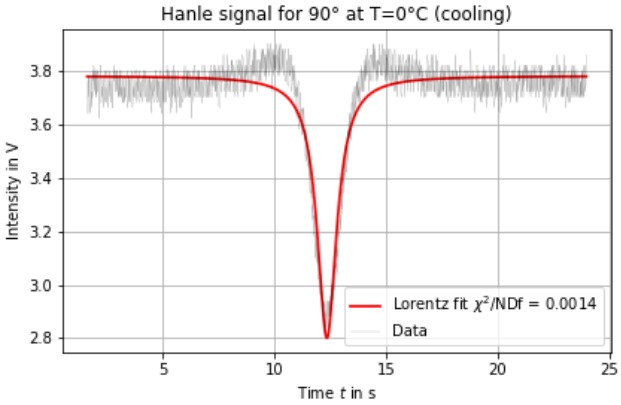
Hanle signal for 90° at T=0°C (cooling)
Intensity in V
Time t in s
Lorentz fit χ^2/NDf = 0.0014
Data

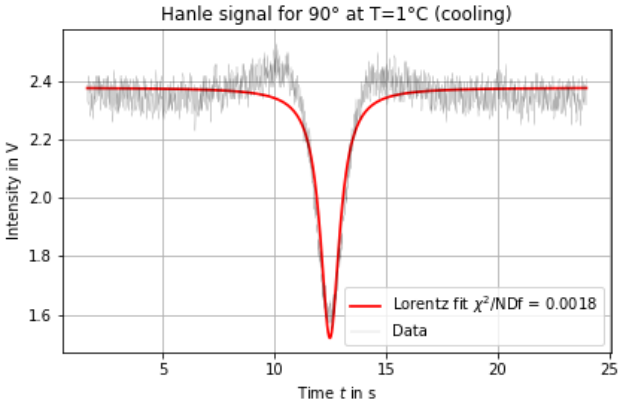
Hanle signal for 90° at T=1°C (cooling)
Intensity in V
Time t in s
Lorentz fit χ^2/NDf = 0.0018
Data

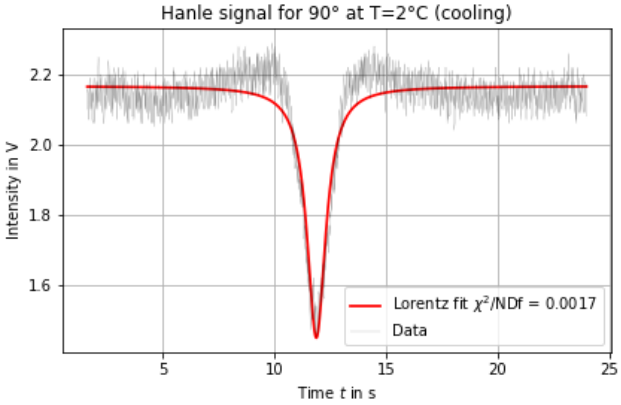
Hanle signal for 90° at T=2°C (cooling)
Intensity in V
Time t in s
Lorentz fit χ^2/NDf = 0.0017
Data

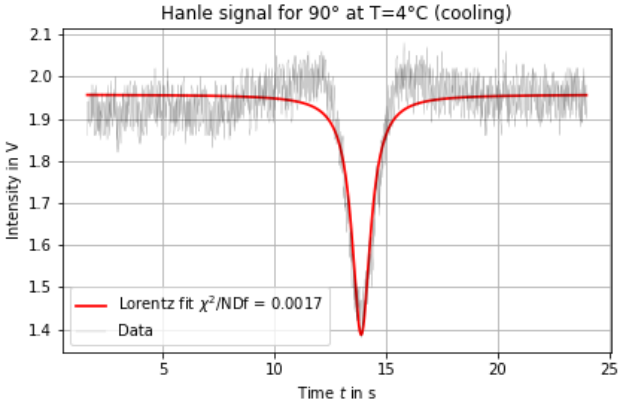
Hanle signal for 90° at T=4°C (cooling)
Intensity in V
Time t in s
Lorentz fit χ^2/NDf = 0.0017
Data

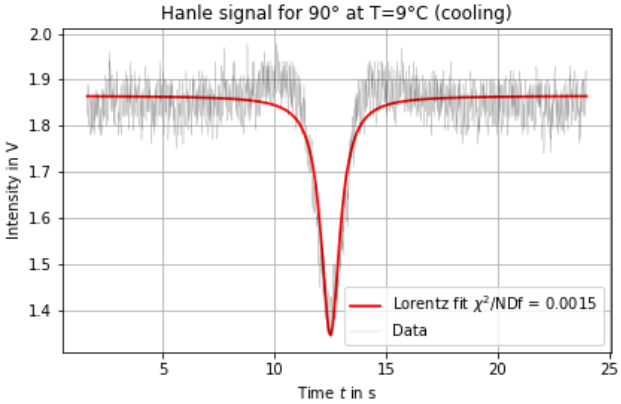
Hanle signal for 90° at T=9°C (cooling)
Intensity in V
Time t in s
Lorentz fit χ^2/NDf = 0.0015
Data

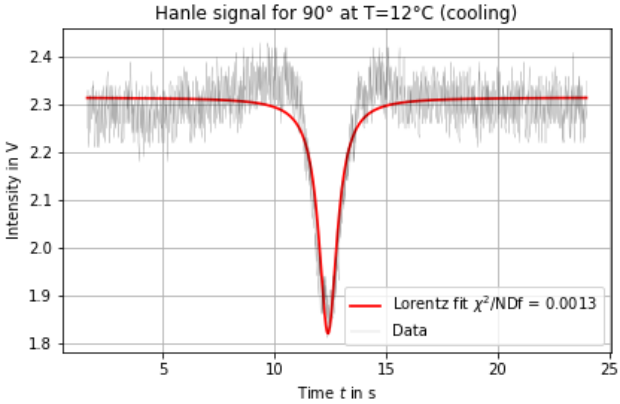
Hanle signal for 90° at T=12°C (cooling)
Intensity in V
Time t in s
Lorentz fit χ^2/NDf = 0.0013
Data

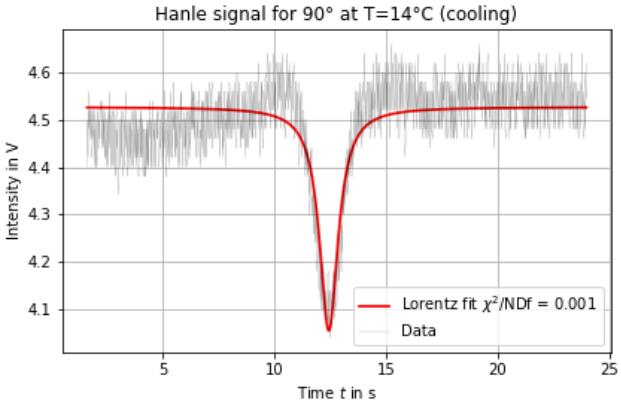

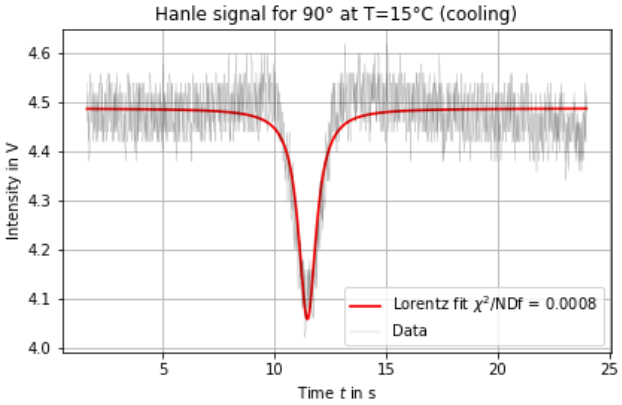

C.2.3 Statistical Measurement

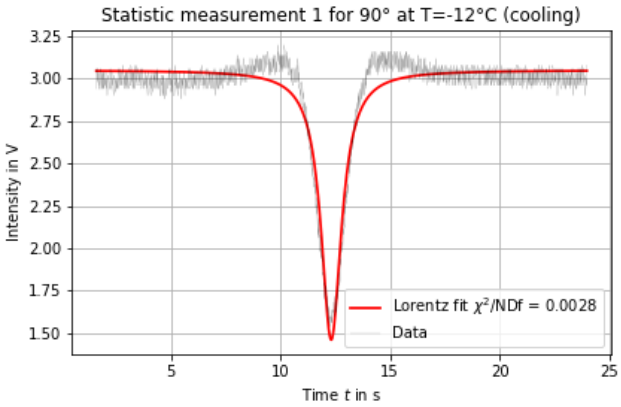

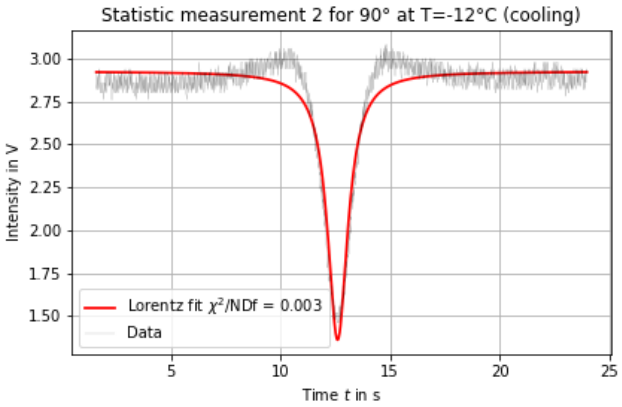

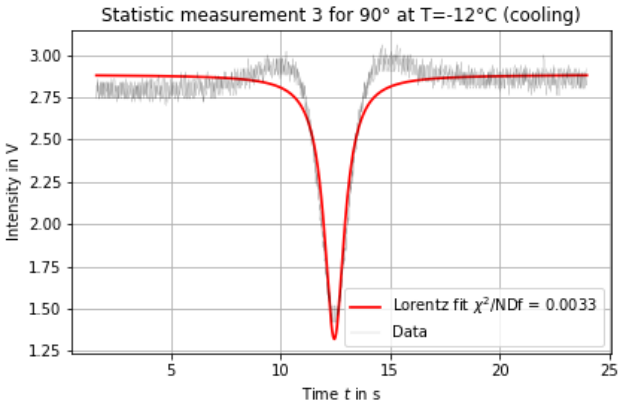

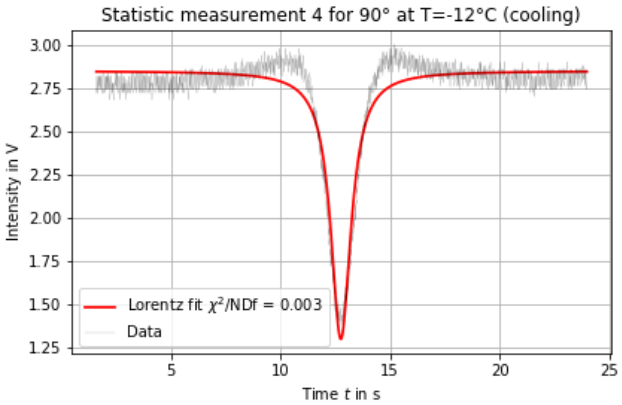

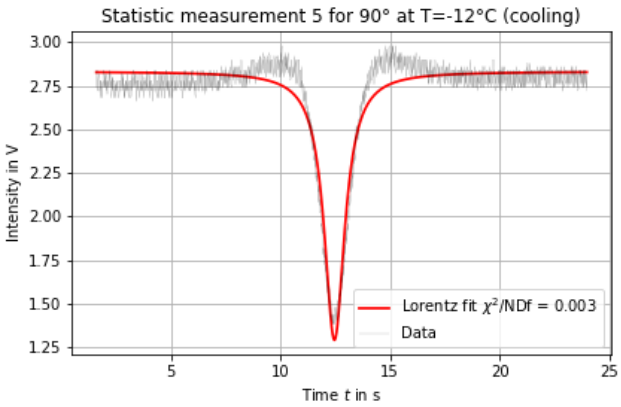
Statistic measurement 5 for 90° at T=-12°C (cooling)
Intensity in V
Time t in s
Lorentz fit χ²/NDf = 0.003
Data

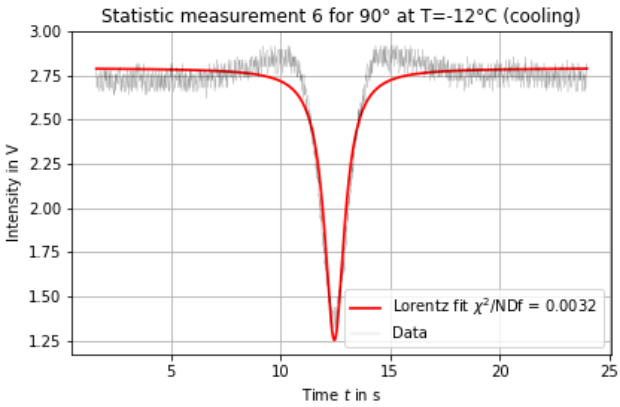
Statistic measurement 6 for 90° at T=-12°C (cooling)
Intensity in V
Time t in s
Lorentz fit χ²/NDf = 0.0032
Data

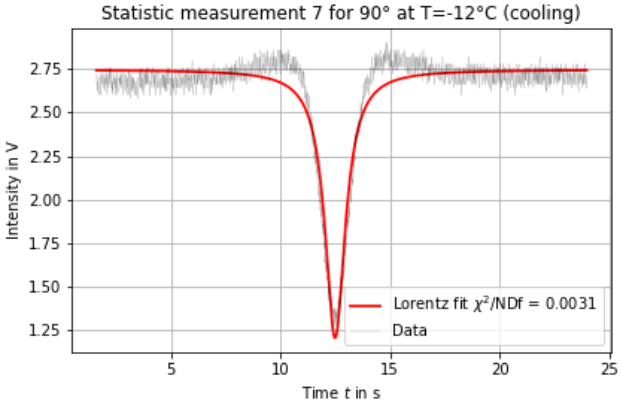
Statistic measurement 7 for 90° at T=-12°C (cooling)
Intensity in V
Time t in s
Lorentz fit χ²/NDf = 0.0031
Data

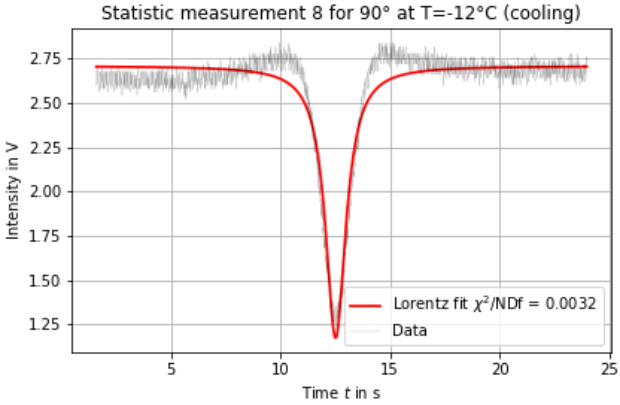
Statistic measurement 8 for 90° at T=-12°C (cooling)
Intensity in V
Time t in s
Lorentz fit χ²/NDf = 0.0032
Data

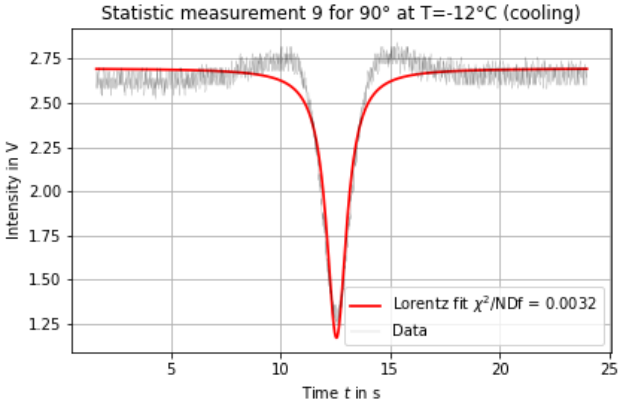
Statistic measurement 9 for 90° at T=-12°C (cooling)
Intensity in V
Time t in s
Lorentz fit χ²/NDf = 0.0032
Data

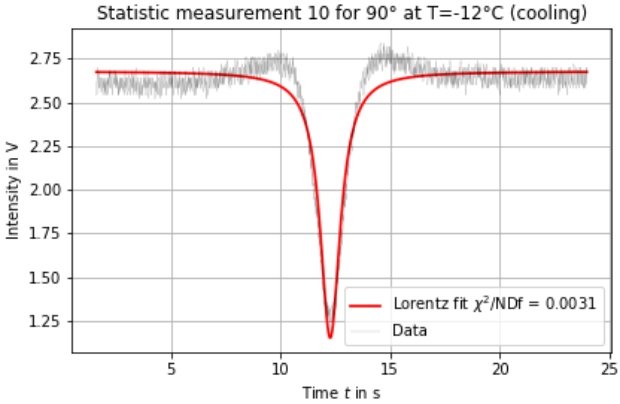
Statistic measurement 10 for 90° at T=-12°C (cooling)
Intensity in V
Time t in s
Lorentz fit χ²/NDf = 0.0031
Data